

Finite-time composite learning control for nonlinear teleoperation systems under networked time-varying delays

Yana YANG*, Huixin JIANG, Changchun HUA & Junpeng LI

Institute of Electrical Engineering, Yanshan University, Qinhuangdao 066004, China

Received 26 September 2023/Revised 27 October 2023/Accepted 17 November 2023/Published online 16 May 2024

Abstract The robust finite-time synchronization control problem is investigated for master-slave networked nonlinear telerobotics systems (NNTSs) in this article. Although there have been some research achievements on finite-time control for the NNTSs, these studies are based on the strong assumptions of communication time delays or can only achieve finite-time bounded convergence even when the external forces are zero. Accordingly and in view of the importance of these issues, a novel robust composite learning adaptive control scheme rendering the finite-time master-slave synchronization is proposed in this paper. In particular, the influence of time delays on finite-time convergence of the system is analyzed by employing the multi-dimension finite-time small-gain framework. Meanwhile, in order to achieve accurate and fast estimation of uncertain parameters of the system, both the online historical and the instantaneous data of the estimation data are explored to derive the new parameter adaptive law under a more realizable interval-excitation (IE) condition. Therefore, the convergence of the position/force synchronization errors and the adaptive parameter estimation errors is obtained in finite time, and enhanced robustness of the closed-loop system will also be ensured. Finally, the superior performance of the proposed control algorithms is validated by numerical simulations and hardware experiments.

Keywords networked teleoperation systems, finite-time control, exact parameter estimation, small-gain theorem, unknown communication delays

1 Introduction

1.1 Background

As a class of typical human-machine interaction systems, networked nonlinear telerobotics systems (NNTSs) have been widely studied and applied all around the world in the last five decades. It is also observed that compared with a fully automated system, the NNTSs are more intelligent as humans joining in command [1]. In practice, as we all know, the unknown time-varying delays during the network transmission can destabilize NNTSs [2, 3]. Thereby, a number of control approaches for NNTSs under time-varying delays are proposed. However, in these studies, only infinite time synchronization performance can be achieved [4–7]. Intuitively, the convergence time and convergence accuracy of the system are two important performance indices for practical NNTSs. It is worth noting that, although there have been some research achievements on finite-time control for the teleoperation systems, these studies are based on the strong assumption of time delays. Besides, these studies ignore the significance of delay-dependent stability conditions for the teleoperation systems. Besides, considering the system uncertainties, due to the poor parameter estimation performance, the existing studies can only achieve finite-time bounded convergence even when the external forces (the forces exerted by human operators and the environment) are zero.

* Corresponding author (email: yyn@ysu.edu.cn)

1.2 Related work

A review of literature yielding numerous finite-time control methods have been proposed for the robot manipulators systems [8–10]. Different from the single robot system, the NNTSs are composed of the master side and the slave side, which are connected with each other by the network communication channel. It results that these existing control schemes designed in [8–10] and the references therein cannot be applied directly to control of the NNTSs. Thereupon, the finite-time control for the NNTSs under constant time-delay is presented in our earlier articles [11,12] and recent article [13]. Furthermore, considering the time variability of networked time delays, some new finite-time control results are also presented [14–20]. In [14], nonsmooth generalized switched filters-based finite-time control methods are proposed to achieve state-independent input-to-output practical stability. Ref. [15] developed a finite-time control approach ensuring that the synchronization errors converge to a residual set, which can be pre-set by the user. By using neural networks, the finite-time boundedness of the NNTSs is proven in [16,17]. A quasi-P+d (proportional plus damping) control method is designed for NNTSs; delay-dependent stability conditions are provided in [18] without taking the system uncertainties into account. Ref. [19] designed a new finite-time controller by combining the position and force synchronization errors; yet the influence of linear filter on finite-time convergence is ignored. Under the physical constraints, the linear filter is applied to avoid the usage of the derivative of time-varying delays when designing the finite-time controller in [20].

It is observed in above literature that, on the one hand, signals related to uncertain communication delays are estimated as uncertainty, as a result, the system becomes more conservative [14,17,19]. On the other hand, even if the external forces are zero, the synchronization error of the system can only converge to the neighborhood of zero due to the lack of real value information of the learned parameters in the learning law [14,17,19,20]. Therefore, although the finite-time control techniques for the NNTSs have been developing, how to fully explore the influence of uncertain communication delays on system stability, and guarantee the estimation speed and accuracy of the uncertain learning parameters under the uncertainties of the system model are still open issues and challenging.

In practical engineering systems, system uncertainty problems inevitably exist. In the methods of system uncertainty estimation, intelligent learning techniques such as neural networks (NNs) or fuzzy logic systems (FLs) have been widely accepted [21–23], the complication in the training of neural weights and fuzzy rules attends a difficulty in practical implementation. Considering the above problem, as a classical method to deal with system uncertainty, parameter estimation methods still play an important role and have been recognized by many research scholars. However, similar with the system tracking performance, the parameter convergence speed and accuracy are two important performance indicators in parameter adaptive control systems [24]. Superior parameter convergence performance will ensure accurate online parameters approximation, accurate trajectory tracking, and strong robustness with parameter drift [25–27]. However, few existing studies concern the issue of parameters convergence speed and accuracy. To solve this problem, the finite-time parameter estimation result is proposed in [28] under the well-known persistent excitation (PE) condition. However, the PE condition is often not realizable in practice. Recently, the finite-time kinematics parameter estimation is shown in [29] under interval-excitation (IE) condition. Compared with PE condition, the IE is a much weaker condition. Considering the uncertain dynamics parameters in robot control, the first composite parameter learning result under the IE condition is proposed in [24]. The main characteristic of composite learning lies in the application of online historical data. However, the parameter estimation errors exponentially converge to zero as time goes infinity in [25]. Intuitively, it is more desirable that accurate parameter estimation is also achieved in finite time under the IE condition [30].

Focusing on above problems, this paper is the first fruitful effort to investigate the finite-time delay-dependent control of the NNTSs with unknown time-varying delays and system uncertainties. Thereby it provides a different insight on how to ensure the fast convergence for a more general networked nonlinear systems. There are two main innovations in this paper.

(1) This paper addresses the delay-dependent stability control problem for a class of uncertain teleoperation systems under time-varying communication delays. Compared with the existing studies [14–20], the communication transmission time-delays considered in this paper are closer to real network communication delays, which could reduce the conservatism of the results.

To relax the assumption of system communication delays, different from the existing control structure, we innovatively split the original closed-loop NNTSs into two subsystems. Then for the first subsystem,

a new CLFTAC scheme is designed by applying a proper Lyapunov function under a recursive structure. Additionally, for the second subsystem, the finite-time convergence is proven by employing the multi-dimension finite-time small-gain theorem. Thus, the finite-time stability of the whole closed-loop NNTSs can be realized. Additionally, the relationship among the controller gains and the maximum of the time-varying delays' derivatives is established by employing the Lyapunov function and the multi-dimension finite-time small-gain theorem.

(2) The closed-loop system control performance is improved by ensuring both the synchronization errors between the master and the slave and the adaptive parameter learning errors to converge to zero with faster convergence speed and higher precision in finite time.

To improve the robustness of the closed-loop NNTSs under the existence of system uncertainty, this paper provides a new result of finite-time system parameter convergence without the PE condition for adaptive control of teleoperation system. The parameter estimation performance is improved by exploring both the online historical and the instantaneous data under a more realizable IE condition. In particular, a forgetting factor is added to adjust the effect of the online historical data and nonlinear filter with fractional powers to speed up signal processing speed.

The rest of our article includes the following sections. In Section 2, some preliminaries on the teleoperation dynamics model and finite-time control theory are given. In Section 3, the detailed controller design process and rigorous theoretical proof are presented. The simulation and experimental validation results are provided in Section 4. Finally, in Section 5 the conclusion is presented.

Notation. $\mathbb{R} = (-\infty, +\infty)$, $\mathbb{R}_+ = (0, +\infty)$ denote the set of real numbers and positive real numbers, respectively. The set of n row k column matrices is given by $\mathbb{R}^{n \times k}$. Also for a vector $H \in \mathbb{R}^n$, $|H|$ denotes element-wise absolute value of H and $\|\cdot\|$ represents the Euclidean 2-norm of H . $\text{sig}(H)^\alpha = [|h_1|^\alpha \text{sign}(h_1), \dots, |h_n|^\alpha \text{sign}(h_n)]^T$, where $H = [h_1, \dots, h_n]^T \in \mathbb{R}^n$, $\alpha \in \mathbb{R}_+$, and $\text{sign}(\cdot)$ represents the standard signum function. For two functions $\chi(\varsigma)$ and $\bar{\chi}(\varsigma)$, there exists $c_1\chi(\varsigma) \leq \bar{\chi}(\varsigma) \leq c_2\chi(\varsigma)$ (when $\|\varsigma\|$ is sufficiently small) with some constants c_1 and c_2 . $\lambda_{\max}(H)$ and $\lambda_{\min}(H)$ are the maximum and minimum eigenvalues of H . $\min(\cdot)$ represents the minimum value of \cdot . $i = m$ is the master and $i = s$ denotes the slave, and $j = 1, 2, \dots, n$ denotes the j th term of a vector.

2 Preliminaries

Consider a nonlinear n -degree of freedom (DOF) human-robot NNTSs as

$$\begin{cases} \mathcal{M}_m(q_m)\ddot{q}_m + \mathcal{C}_m(q_m, \dot{q}_m)\dot{q}_m + \mathcal{G}_m(q_m) + \mathcal{F}_m = \tau_m + \mathcal{F}_h, \\ \mathcal{M}_s(q_s)\ddot{q}_s + \mathcal{C}_s(q_s, \dot{q}_s)\dot{q}_s + \mathcal{G}_s(q_s) + \mathcal{F}_s = \tau_s - \mathcal{F}_e, \end{cases} \quad (1)$$

where $q_i(t)$, $\dot{q}_i(t)$, $\ddot{q}_i(t) \in \mathbb{R}^n$ are the vectors of the joint displacements, velocities, and accelerations with $i = m, s$; $\mathcal{M}_i(q_i) = \mathcal{M}_{io}(q_i) + \Delta\mathcal{M}_i(q_i) \in \mathbb{R}^{n \times n}$ are the inertia matrices; $\mathcal{C}_i(q_i, \dot{q}_i) = \mathcal{C}_{io}(q_i, \dot{q}_i) + \Delta\mathcal{C}_i(q_i, \dot{q}_i) \in \mathbb{R}^{n \times n}$ are the matrices of Centripetal and Coriolis terms; $\mathcal{G}_i(q_i) = \mathcal{G}_{io}(q_i) + \Delta\mathcal{G}_i(q_i) \in \mathbb{R}^n$ are the gravitational torques; $\mathcal{F}_i = \bar{\mathcal{F}}_i + d_i$ contains the bounded external disturbances d_i which are caused by low-frequency load disturbances and set point changes and satisfies $\|d_i\| \leq \bar{d}_i$, where \bar{d}_i is a positive constant, and frictions $\bar{\mathcal{F}}_i$ take the Coulomb friction, static friction, viscous friction, and Stribeck effect into account [31], given as $\bar{\mathcal{F}}_i = \gamma_{i1}(\tanh(\gamma_{i2}\dot{q}_i) - \tanh(\gamma_{i3}\dot{q}_i)) + \gamma_{i4} \tanh(\gamma_{i5}\dot{q}_i) + \gamma_{i6}\dot{q}_i$, $\gamma_{i1} \sim \gamma_{i6}$ all are positive constants; $\mathcal{F}_h \in \mathbb{R}^n$ is the human operator inserted torque and $\mathcal{F}_e \in \mathbb{R}^n$ is external environmental torque; $\tau_i \in \mathbb{R}^n$ are the designed control torques. Here $\mathcal{M}_{io}(q_i)$, $\mathcal{C}_{io}(q_i, \dot{q}_i)$, $\mathcal{G}_{io}(q_i)$ are the nominal parts, whereas the perturbations in the system matrices are given as $\Delta\mathcal{M}_i(q_i)$, $\Delta\mathcal{C}_i(q_i, \dot{q}_i)$, $\Delta\mathcal{G}_i(q_i)$. Then system (1) can be rearranged as

$$\mathcal{M}_{io}(q_i)\ddot{q}_i + \mathcal{C}_{io}(q_i, \dot{q}_i)\dot{q}_i + \mathcal{G}_{io}(q_i) = \tau_i - F_i(q_i, \dot{q}_i, \ddot{q}_i) - d_i + \mathcal{F}_{ihe}, \quad (2)$$

where $\mathcal{F}_{mhe} = \mathcal{F}_h$, $\mathcal{F}_{she} = -\mathcal{F}_e$, and $F_i(q_i, \dot{q}_i, \ddot{q}_i) = \Delta\mathcal{M}_i(q_i)\ddot{q}_i + \Delta\mathcal{C}_i(q_i, \dot{q}_i)\dot{q}_i + \Delta\mathcal{G}_i(q_i) + \bar{\mathcal{F}}_i$ are viewed as the lumped system uncertainties, which can be derived based on (1) and (2).

The following common properties of system (1) with revolute joints are presented [4-7].

Property 1. The symmetric positive-definite matrix $\mathcal{M}_{io}(q_i)$ satisfies $\lambda_{\min}(\mathcal{M}_{io}(q_i)) \leq \|\mathcal{M}_{io}(q_i)\| \leq \lambda_{\max}(\mathcal{M}_{io}(q_i))$.

Property 2. Dynamics (1) is linearly parameterizable,

$$\mathcal{M}(q)\xi + \mathcal{C}(q, \dot{q})\eta + \mathcal{G}(q) = Y(q, \dot{q}, \xi, \eta)\theta, \tag{3}$$

where $Y(q, \dot{q}, \xi, \eta) \in \mathbb{R}^{n \times \kappa}$ denotes a regressor matrix, θ is a κ -dimensional vector of unknown constant parameters.

The positions $q_i(t)$ and velocities $\dot{q}_i(t)$ of system are assumed to be measurable and the control objective of this paper is to propose a novel delay-dependent finite-time control algorithm for the uncertain NNTSs (1) with unknown asymmetric time-varying delays. With the designed control scheme, the joint position synchronization errors $q_m - q_s(t - T_s(t))$, $q_s - q_m(t - T_m(t))$ and the joint velocities \dot{q}_m , \dot{q}_s converge to zero in finite time when \mathcal{F}_h and \mathcal{F}_e are zero, where $T_m(t)$ and $T_s(t)$ are the signal transmission delays from the local side to the remote side and that in opposite direction, respectively. Finally, the result that $q_m - q_s = 0$ can be achieved in finite time. Besides, the modified direct-force-feedback finite-time control method is also designed to provide improved transparency performance.

Assumption 1. Time delays $T_i(t) : \mathbb{R}_+ \rightarrow \mathbb{R}_+$ ($i = m, s$) satisfies some properties as follows:

- (1) $|T_i(t)| \leq T^*(t)$, where $T^*(t) : \mathbb{R}_+ \rightarrow \mathbb{R}_+$ and for all $t_1, t_2 \in \mathbb{R}_+$, the inequality $T^*(\bar{t}_2) - T^*(\bar{t}_1) \leq \bar{t}_2 - \bar{t}_1$ holds for all $t > 0$;
- (2) the equation $t - T_i(t) \rightarrow +\infty$ holds when $t \rightarrow +\infty$;
- (3) $|T_i(\bar{t}_2) - T_i(\bar{t}_1)| \leq \Upsilon_i |\bar{t}_2 - \bar{t}_1|$, where $\Upsilon_i \in \mathbb{R}_+$, $\bar{t}_2 > \bar{t}_1$, and almost all $\bar{t}_2, \bar{t}_1 \in \mathbb{R}_+$.

Remark 1. On the one hand, Assumption 1 on time-delays implies that there exists a maximum $T^*(t)$. Moreover, the function $T^*(t)$ can be chosen to be unbounded and time-varying; i.e., there is no requirement of the value of $T^*(t)$ but the $T^*(t)$ cannot grow faster than the time itself. On the other hand, $dT_i(t)/dt$ satisfies $|dT_i(t)/dt| \leq \Upsilon_i$ for almost all $t \geq 0$. In [15], the authors claimed that $\dot{z}_{i1} = \ddot{x}_{i1} - \dot{\rho}_{i1} = \dot{x}_{i2} - \dot{\rho}_{i1}$, i.e., $\ddot{x}_{i1} = \dot{x}_{i2}$ with $x_{m1} = q_m(t) - q_s(t - T_s)$ and $x_{m2} = \dot{q}_m(t) - \dot{q}_s(t - T_s)$, $i = m$. It is obvious that $\ddot{x}_{m1} = \ddot{q}_m(t) - (1 - \dot{T}_s)\ddot{q}_s(t - T_s) + \dot{T}_s\dot{q}_s(t - T_s) + \dot{T}_s(1 - \dot{T}_s)\dot{q}_s(t - T_s)$ and $\dot{x}_{m2} = \dot{q}_m(t) - (1 - \dot{T}_s)\dot{q}_s(t - T_s)$. To ensure $\ddot{x}_{i1} = \dot{x}_{i2}$, the forward and backward time delays T_m and T_s must be constant. The time delay $T_i(t)$ and its change rate $\dot{T}_i(t)$ are assumed to be less than fixed constants (which can be seen in the Assumption 2 in [16], the Assumption 3 in [17], the Assumption 2 in [20], and the Assumption 4 in [14]). And the time-delay $T_i(t)$ is assumed to be bounded (which can be seen in the Assumption 1 in [18]). Therefore, it is evident that compared with [16–20], the assumption on the upper bound of time delays is reduced in this paper. Therefore, Assumption 1 given in this paper is much weaker.

Assumption 2. It is assumed that the exerted forces \mathcal{F}_h and \mathcal{F}_e are bounded.

Definition 1 ([32]). Consider a nonlinear dynamical system shown as follows:

$$\dot{x} = g(x), \quad g(0) = 0, \quad x \in \mathbb{R}^n, \tag{4}$$

where the function $g : \Lambda_0 \rightarrow \mathbb{R}^n$ is continuous in an open neighborhood Λ_0 around the origin. If the system (4) is Lyapunov stable and finite-time convergent in neighborhood $\Lambda \subset \Lambda_0$ around the origin, then it concludes that the system (4) is (locally) finite-time stable with equilibrium $x = 0$. The finite-time convergence means $\forall x_0 \in \Lambda \subset \mathbb{R}^n$, there exists a function $T : \Lambda \setminus \{0\} \rightarrow (0; \infty)$, with x_0 as the initial condition, the solution of (4) $s_t(x_0)$ satisfies $s_t(x_0) \in U \setminus \{0\}$ for $t \in [0; T(x_0))$, and $\lim_{t \rightarrow T(x_0)} s_t(x_0) = 0$ with $s_t(x_0) = 0$ for $t > T(x_0)$. Moreover, if $\Lambda = \mathbb{R}^n$, the global finite-time stability (FTS) can be ensured.

Definition 2 ([33]). For a continuous function $\zeta : \mathbb{R}_+ \rightarrow \mathbb{R}_+$, if it is strictly increasing with $\zeta(0) = 0$, then ζ belongs to class \mathcal{K} ($\zeta \in \mathcal{K}$). Moreover, for a function $\zeta \in \mathcal{K}$ with $\zeta(\varpi) \rightarrow \infty$ as $\varpi \rightarrow \infty$, then ζ also belongs to class \mathcal{K}_∞ . Class $\bar{\mathcal{K}}$ is defined as $\bar{\mathcal{K}} := \mathcal{K} \cup \{0\}$; $\mathcal{O}(\varpi) \equiv 0$ for all $\varpi \geq 0$ is a zero function. A function $\zeta : \mathbb{R}_+ \times \mathbb{R}_+ \rightarrow \mathbb{R}_+$ is of class \mathcal{KL} , if for each fixed $t \in \mathbb{R}_+$ in the first argument $\zeta(\cdot, t) \in \mathcal{K}$ and for each fixed $\varpi \geq 0$, $\zeta(\varpi, t)$ decreases to 0 as $t \rightarrow +\infty$.

Definition 3 ([34]). A function $\vartheta : \mathbb{R}_+ \rightarrow \mathbb{R}_+$ belongs to the class generalized \mathcal{K} (\mathcal{GK}) function if ϑ is continuous with $\vartheta(0) = 0$, and

$$\begin{cases} \vartheta(r_1) > \vartheta(r_2), & \text{if } \vartheta(r_1) \neq 0, \\ \vartheta(r_1) = \vartheta(r_2), & \text{if } \vartheta(r_1) = 0 \end{cases} \tag{5}$$

hold for any $r_1 > r_2$. A function $\zeta : \mathbb{R}_+ \times \mathbb{R}_+ \rightarrow \mathbb{R}_+$ belongs to the class generalized \mathcal{KL} function (\mathcal{GKL}) if $\zeta(\varpi, t)$ is a \mathcal{GK} function for each fixed $t \geq 0$, and for each fixed $\varpi \geq 0$ decreases to zero as $t \rightarrow T$ for some $T \leq \infty$, which is called the settling time of \mathcal{GKL} -function $\zeta(\cdot, \cdot)$.

In Definition 3, it is clear that a (conventional) class \mathcal{K} function is a class \mathcal{GK} function. For the following nonlinear system:

$$\begin{aligned} \dot{\eta} &= f(\eta) + g_1(\eta)u_1 + \cdots + g_q(\eta)u_q, \\ y_1 &= h_1(\eta), \dots, y_p = h_p(\eta), \end{aligned} \tag{6}$$

where $\eta \in \mathbb{R}^N$, $u_i \in \mathbb{R}^{m_i}$ for $i \in \mathcal{N}_q := (1, \dots, q)$, $y_j \in \mathbb{R}^{m_j}$ for $j \in \mathcal{N}_p := (1, \dots, p)$, $f(\cdot)$ and $g_i(\cdot)$ are locally Lipschitz functions for $a \in \mathcal{N}_p$ and $h_j(\cdot)$ for $j \in \mathcal{N}_q$, and their initial values are zero. For any $\eta(t_0)$ and any $u_1(t), \dots, u_q(t)$ that are uniform essentially bounded on $[t_0, t_1]$, the $\eta(t)$ is well defined for all $t \in [t_0, t_1]$.

Next, the definitions for weakly finite-time input-to-state stable (WFTISS) and weakly finite-time input-to-output stable (WFTIOS) are presented.

Definition 4. Consider the system (6), if for any $\eta(t_0)$ and measurable uniformly essentially bounded inputs u_i ($i \in \mathcal{N}_q$), the $\eta(t)$ is well-defined for all $t \geq t_0$ and satisfies

(1) uniform boundedness:

$$\|x(t)\| \leq \zeta(\|x(t_0)\|, t) + \gamma_i \left(\sup_{s \in [t_0, t]} \|u_i(s)\| \right), \tag{7}$$

(2) finite-time gain:

$$\limsup_{t \rightarrow T(r)} \|x(t)\| \leq \gamma_i \left(\limsup_{t \rightarrow T(r)} \|u(t)\| \right), \tag{8}$$

where the function ζ belongs to \mathcal{GKL} with $\zeta(\varpi, t) \equiv 0$ when $t \geq T(\varpi)$, $\gamma_i \in \mathcal{K}$ with $i \in \mathcal{N}_q$. Then the system (6) is said to be WFTISS. Additionally, the system (6) is said to be WFTIOS if $\forall t_0, t \in \mathbb{R}_+$, $t \geq t_0$, the following inequality

$$\|y_i(t)\| \leq \zeta_i(\|x(t_0)\|, t) + \bar{\gamma}_{ij} \left(\sup_{s \in [t_0, t]} \|u_j(s)\| \right) \tag{9}$$

holds with $\zeta_i \in \mathcal{GKL}$, $\zeta_i(\varpi, t) \equiv 0$, $i \in \mathcal{N}_q$ when $t \geq \bar{T}(\varpi)$, and $\bar{\gamma}_{ij} \in \mathcal{K}$ with $i \in \mathcal{N}_q, j \in \mathcal{N}_p$.

Lemma 1 (Multi-dimension finite-time small-gain theorem). For a system under the form (6), when the system is WFTIOS with linear WFTIOS gain $\gamma_{ij}^0 \geq 0$ and each input $u_i(\cdot)$, $j \in \mathcal{N}_q$, is a Lebesgue measurable function satisfying

$$u_i(t) \equiv 0 \text{ for } t < 0 \tag{10}$$

and

$$\|u_i(t)\| \leq \sum_{j \in \mathcal{N}_q} \mu_{ji} \cdot \sup_{s \in [t - T_{ij}(t), t]} \|y_j(s)\| \tag{11}$$

for almost all $t \geq 0$, where $\mu_{ji} \geq 0$ and time-delays $T_{ij}(t)$ satisfy Assumption 1. Define $\Gamma := \Gamma^0 \cdot \mathcal{M} \in \mathbb{R}^{q \times q}$ with $\Gamma^0 := \{\gamma_{ij}^0\}$, $\mathcal{M} := \{\mu_{ji}\}$, $i \in \mathcal{N}_q, j \in \mathcal{N}_p$. If the spectral radius of the matrix Γ named $\rho(\Gamma)$ is less than 1, then all the output $y_j(t)$ of system (6), $i \in \mathcal{N}_p$ and all the input $u_i(t)$, $i \in \mathcal{N}_p$ are uniformly bounded and satisfy $\|y_j(t)\| \rightarrow 0, \|u_i(t)\| \rightarrow 0$ as $t \rightarrow T(x_0)$ for all $t > 0$.

In this paper, the multi-dimension finite-time small-gain theorem is first raised. Based on [33, 34], the detailed proof process of Lemma 1 is shown in Appendix A.

Definition 5 ([24]). For signal $\Phi(t) \in \mathbb{R}^N$, which is bounded, if during $t \in [T_d - \bar{\tau}, T_d]$, such that $\int_{T_d - \bar{\tau}}^{T_d} \Phi^T(\tau)\Phi(\tau)d\tau \geq \bar{\epsilon}I$ with constants $T_d, \bar{\tau}, \bar{\epsilon} \in \mathbb{R}_+$, then $\Phi(t)$ is of IE. And if $\int_{t - \bar{\tau}}^t \Phi^T(\tau)\Phi(\tau)d\tau \geq \epsilon I, \forall t \geq 0$, then $\Phi(t)$ is of PE.

Lemma 2 ([12]). Letting $\delta_1, \delta_2, \dots, \delta_n \geq 0$, if $\rho > 0$ then

$$\delta_1^\rho + \delta_2^\rho + \cdots + \delta_n^\rho \geq (\delta_1 + \delta_2 + \cdots + \delta_n)^\rho. \tag{12}$$

When $\rho = \frac{a_1}{a_2} \leq 1$ with $a_1, a_2 \in \mathbb{R}_+$ being odd integers, then $|x_1^\rho - x_2^\rho| \leq 2^{1-\rho} |x_1 - x_2|^\rho$.

Lemma 3 ([35]). Letting α_1, α_2 be positive real numbers and $r(\zeta_1, \zeta_2)$ be a real-valued function, it has

$$|\zeta_1|^{\alpha_1} |\zeta_2|^{\alpha_2} \leq \frac{\alpha_1 r(\zeta_1, \zeta_2) |\zeta_1|^{\alpha_1 + \alpha_2}}{\alpha_1 + \alpha_2} + \frac{\alpha_2 r^{-\frac{\alpha_1}{\alpha_2}}(\zeta_1, \zeta_2) |\zeta_2|^{\alpha_1 + \alpha_2}}{\alpha_1 + \alpha_2}. \tag{13}$$

3 Controller design and stability analysis

Letting $x_{i1} = q_i$, $x_{i2} = \dot{q}_i$, the function (2) can be rearranged as the following strict-feedback form:

$$\begin{aligned} \dot{x}_{i1} &= x_{i2}, \\ \dot{x}_{i2} &= -\mathcal{M}_{io}^{-1}(x_{i1})(\mathcal{C}_{io}(x_{i1}, x_{i2})x_{i2} + \mathcal{G}_{io}(x_{i1}) + F_i(x_{i1}, x_{i2}, \dot{x}_{i2}) + d_i - \tau_i - \mathcal{F}_{ihe}). \end{aligned} \quad (14)$$

Let us propose new auxiliary variables ψ_{i1} , ψ_{i2} , which satisfy

$$\dot{\psi}_{i1} = \psi_{i2}, \quad \dot{\psi}_{i2} = f(\tilde{\psi}_{i1}, \psi_{i2}), \quad (15)$$

where $f(\tilde{\psi}_{i1}, \psi_{i2})$ denotes the nonlinear functions of $\tilde{\psi}_{i1}$ and ψ_{i2} , which will be designed later.

With the above variables, define error variables $e_{i1} = x_{i1} - \psi_{i1}$, $e_{i2} = x_{i2} - \psi_{i2}$. Applying Property 2 of system (2) and the definition of friction term, the following equation can be achieved directly:

$$\begin{aligned} \dot{e}_{i1} &= e_{i2}, \\ \dot{e}_{i2} &= -\mathcal{M}_{io}^{-1}(x_{i1})(\mathcal{C}_{io}(x_{i1}, x_{i2})x_{i2} + \mathcal{G}_{io}(x_{i1}) + Y_i(x_{i1}, x_{i2}, \dot{x}_{i2})\theta_i + d_i - \tau_i - \mathcal{F}_{ihe}) - \dot{\psi}_{i2}, \end{aligned} \quad (16)$$

where $\dot{\psi}_{i2}$ denote the derivative of ψ_{i2} .

With the introduced auxiliary variables ψ_{i1} , ψ_{i2} , the original teleoperation system (1) can be divided into two subsystems (15) and (16). Then, τ_i and $f(\tilde{\psi}_{i1}, \psi_{i2})$ will be designed to ensure finite-time stability of these two subsystems. For the subsystem (16), based on the designed error variables e_{i1} and e_{i2} , the CLFTAC scheme will be proposed by developing a recursive structure firstly.

Step 1. Construct a Lyapunov function candidate $V_1 = \sum_{i=m,s} e_{i1}^T e_{i1}$, which yields

$$\dot{V}_1 = \sum_{i=m,s} e_{i1}^T (e_{i2} - e_{i2}^*) + e_{i1}^T e_{i2}^*, \quad (17)$$

where e_{i2}^* are virtual control variables designed as $e_{i2}^* = -k_{i1} \text{sig}(e_{i1})^{\rho_1}$, $k_{i1} \in \mathbb{R}_+$, $1/2 < \rho_1 = \frac{a_1}{a_2} < 1$, and $a_1, a_2 \in \mathbb{R}_+$ are odd integers. Thus we have

$$\begin{aligned} \dot{V}_1 &= \sum_{i=m,s} e_{i1}^T (e_{i2} - e_{i2}^*) - k_{i1} e_{i1}^T \text{sig}(e_{i1})^{\rho_1} \\ &\leq \sum_{i=m,s} - \left(k_{i1} - \frac{1}{2} \right) \|e_{i1}\|^{1+\rho_1} + c_{i1} \left\| e_{i2}^{1/\rho_1} - e_{i2}^{*/\rho_1} \right\|^{1+\rho_1} \end{aligned} \quad (18)$$

where $(e_{i2j} - e_{i2j}^*) = ((e_{i2j}^{1/\rho_1})^{\rho_1} - (e_{i2j}^{*/\rho_1})^{\rho_1}) = 2^{1-\rho_1} (e_{i2j}^{1/\rho_1} - e_{i2j}^{*/\rho_1})^{\rho_1}$ by applying Lemma 2, and e_{i2j} and e_{i2j}^* denote the j th term of vectors e_{i2j} and e_{i2j}^* , respectively. Then according to Lemma 3, it has

$$e_{i1}^T (e_{i2} - e_{i2}^*) \leq \frac{1}{2} \|e_{i1}\|^{1+\rho_1} + c_{i1} \|e_{i2}^{1/\rho_1} - e_{i2}^{*/\rho_1}\|^{1+\rho_1} \text{ with } c_{i1} = \frac{\rho_1 2^{(2-\rho_1)/\rho_1}}{(1+\rho_1)^{(1+\rho_1)/\rho_1}}.$$

Step 2. Let us define $\xi_i = e_{i2}^{1/\rho_1} - e_{i2}^{*/\rho_1}$ and

$$\begin{aligned} \bar{V}_2 &= V_1 + \sum_{i=m,s} \sum_{j=1}^n \int_{e_{i2j}^*}^{e_{i2j}} (s^{1/\rho_1} - e_{i2j}^{*/\rho_1})^{2-\rho_1} ds + \sum_{i=m,s} \frac{1}{2} \tilde{\theta}_i^T \Lambda_i^{-1} \tilde{\theta}_i \\ &\quad + \int_0^t (\xi_m^{2-\rho_1})^T Q_m K_F |\mathcal{F}_h + \mathcal{F}_e(t - T_s(t))| dt, \end{aligned} \quad (19)$$

where $Q_m = \text{diag}(\text{sign}(\xi_m) + \varepsilon)$, $\varepsilon = [\varepsilon_1, \varepsilon_2, \dots, \varepsilon_n]^T \in \mathbb{R}^n$ is a vector, whose elements are $0 < \varepsilon_j \ll 1$, $j = 1, 2, \dots, n$, which can ensure the force reflection for $\dot{q}_i \rightarrow 0$. $K_F \in \mathbb{R}^{n \times n}$ is a diagonal positive-definite matrix. Λ_i are diagonal positive-definite matrices. $\tilde{\theta}_i = \hat{\theta}_i - \theta_i$ and $\hat{\theta}_i$ are the estimations for θ_i . It is easy to prove \bar{V}_2 is positive (see [36] for detail).

According to Lemmas 2 and 3, one has

$$\dot{\bar{V}}_2 \leq \sum_{i=m,s} - (k_{i1} - 1) \|e_{i1}\|^{1+\rho_1} + (\xi_i^{2-\rho_1})^T \dot{e}_{i2} + (c_{i1} + c_{i2}) \|\xi_i\|^{1+\rho_1}$$

$$+ \tilde{\theta}_i^T \Lambda_i^{-1} \dot{\hat{\theta}}_i + \left(\xi_m^{\frac{\rho_1+1}{2}} \right)^T Q_m K_F |\mathcal{F}_h + \mathcal{F}_e(t - T_s(t))| \quad (20)$$

where the derivative of $\Pi_i = \sum_{i=m,s} \sum_{j=1}^n \int_{e_{i2_j}^*}^{e_{i2_j}} (s^{1/\rho_1} - e_{i2_j}^{*1/\rho_1})^{2-\rho_1} ds$ is $\dot{\Pi}_i = (\xi_i^{2-\rho_1})^T \dot{e}_{i2} + (2-\rho_1) \frac{d(-e_{i2_j}^{*1/\rho_1})}{dt} \times \int_{e_{i2_j}^*}^{e_{i2_j}} (s^{1/\rho_1} - e_{i2_j}^{*1/\rho_1})^{2-\rho_1} ds$, $\frac{d(-e_{i2_j}^{*1/\rho_1})}{dt} = k_{i1}^{1/\rho_1} (|\xi_{i_j}|^{\rho_1} - k_{i1} \text{sig}(e_{i1_j})^{\rho_1})$, and $|\int_{e_{i2_j}^*}^{e_{i2_j}} (s^{1/\rho_1} - e_{i2_j}^{*1/\rho_1})^{2-\rho_1} ds| = 2^{1-\rho_1} |\xi_{i_j}|$. $c_{i2} = \Xi_i + \frac{(2\rho_1)^{\rho_1} (k_{i1} \Xi_i)^{1+\rho_1}}{(1+\rho_1)^{1+\rho_1}}$ with $\Xi_i = (2-\rho_1) 2^{1-\rho_1} k_{i1}^{1/\rho_1}$.

The novel direct-force-feedback CLFTAC scheme for the master and slave robots is proposed as

$$\begin{aligned} \bar{\tau}_m &= Y_m(x_{m1}, x_{m2}, \dot{x}_{m2}) \hat{\theta}_m + \mathcal{C}_{m0}(x_{m1}, x_{m2}) x_{m2} + \mathcal{G}_{m0}(x_{m1}) - \bar{d}_m \text{sign}(\xi_m) \\ &\quad + \mathcal{M}_{m0}(x_{m1}) (\dot{\psi}_{m2} - k_{m2} \text{sig}(\xi_m)^{\rho_2} - Q_m K_F |\mathcal{F}_h + \mathcal{F}_e(t - T_s(t))|) - \mathcal{F}_h, \\ \bar{\tau}_s &= Y_s(x_{s1}, x_{s2}, \dot{x}_{s2}) \hat{\theta}_s + \mathcal{C}_{s0}(x_{s1}, x_{s2}) x_{s2} + \mathcal{G}_{s0}(x_{s1}) \\ &\quad + \mathcal{M}_{s0}(x_{s1}) (\dot{\psi}_{s2} - k_{s2} \text{sig}(\xi_s)^{\rho_2}) + \mathcal{F}_e - \bar{d}_s \text{sign}(\xi_s), \end{aligned} \quad (21)$$

where $k_{i2} \in \mathbb{R}^{n \times n}$, $\rho_2 \in \mathbb{R}_+$ satisfies $\rho_2 = 2\rho_1 - 1$.

As we can see from the control scheme in (21), the term $Y_i(x_{i1}, x_{i2}, \dot{x}_{i2}) \hat{\theta}_i$ includes acceleration signals \dot{x}_{i2} . In most cases, it is a challenging task to measure the accelerations for a robot manipulator. To avoid using acceleration signals \dot{x}_{i2} in parameter estimation, different from the widely used first-order linear filter, we design the nonlinear filter operation by introducing the power term; i.e., $k \dot{x}_{i2f} = \text{sig}(x_{i2f} - x_{i2})^{\rho_1}$ is designed to approximate \dot{x}_{i2} with $k \in \mathbb{R}_+$. Then \dot{x}_{i2f} will be used instead of the actual acceleration signal \dot{x}_{i2} .

One has the parameters composite learning law as

$$\dot{\hat{\theta}}_i = \Lambda_i \mathcal{P} \left(Y_i^T(x_{i1}, x_{i2}) \mathcal{M}_{i0}^{-1}(x_{i1}) \xi_i^{2-\rho_1} + L_i \text{sig}(W_i(T_d))^{\rho_1} \right), \quad (22)$$

where L_i are diagonal positive-definite matrices, $T_d \in \mathbb{R}_+$ is an integral duration, $W_i(t)$ can be obtained with the nonlinear filter technology shown in Appendix, and a projection operator $\mathcal{P}(\bullet)$ is designed as

$$\mathcal{P}(\bullet) = \begin{cases} \bullet, & \text{if } \|\hat{\varrho}\| < c_\varrho \text{ or } \|\hat{\varrho}\| = c_\varrho \& \hat{\varrho}^T \bullet \leq 0, \\ \bullet - \hat{\varrho} \hat{\varrho}^T \bullet / \|\hat{\varrho}\|^2, & \text{otherwise,} \end{cases}$$

where c_ϱ is a positive constant.

With the above designed control scheme (21) and the system error equation (16), taking the master robot as an example, one has

$$\begin{aligned} (\xi_m^{2-\rho_1})^T \dot{e}_{m2} &= (\xi_m^{2-\rho_1})^T \mathcal{M}_{m0}^{-1}(x_{m1}) Y_m(x_{m1}, x_{m2}, \dot{x}_{m2}) \hat{\theta}_m - (\xi_m^{2-\rho_1})^T k_{m2} \text{sig}(\xi_m)^{\rho_2} \\ &\quad + (\xi_m^{2-\rho_1})^T \mathcal{M}_{m0}^{-1}(x_{m1}) \times (d_m - \bar{d}_m \text{sign}(\xi_m)) - (\xi_m^{2-\rho_1})^T Q_m K_F |\mathcal{F}_h + \mathcal{F}_e(t - T_s(t))|. \end{aligned}$$

Furthermore, we have

$$\begin{aligned} \dot{\bar{V}}_2 &\leq \sum_{i=m,s} \left(-(k_{i1} - 1) \|e_{i1}\|^{1+\rho_1} + (c_{i1} + c_{i2}) \|\xi_i\|^{1+\rho_1} - (\xi_i^{2-\rho_1})^T k_{i2} \text{sig}(\xi_i)^{\rho_2} \right. \\ &\quad \left. + \tilde{\theta}_i (Y_i^T(x_{i1}, x_{i2}) \mathcal{M}_{i0}^{-1}(x_{i1}) \xi_i^{2-\rho_1} + \Lambda_i^{-1} \dot{\hat{\theta}}_i) \right). \end{aligned} \quad (23)$$

By choosing $k_{i1} - 1 = \bar{k}_{i1}$, $k_{i2} - (c_{i1} + c_{i2}) = \bar{k}_{i2}$, $\bar{k}_{i1}, \bar{k}_{i2} \in \mathbb{R}_+$, we then have

$$\dot{\bar{V}}_2 \leq \sum_{i=m,s} \left(-\bar{k}_{i1} \|e_{i1}\|^{1+\rho_1} - \bar{k}_{i2} \|\xi_i\|^{1+\rho_1} + \tilde{\theta}_i (Y_i^T(x_{i1}, x_{i2}) \mathcal{M}_{i0}^{-1}(x_{i1}) \xi_i^{2-\rho_1} - \Lambda_i^{-1} \dot{\hat{\theta}}_i) \right). \quad (24)$$

From the result of the projection operation (see Theorem 4.6.1 in [37]), the adaptive law (22) ensures

$\hat{\theta} \in \Omega_{c_\theta}$ and $\tilde{\theta}_i (Y_i^T(x_{i1}, x_{i2}) \mathcal{M}_{i0}^{-1}(x_{i1}) \xi_i^{2-\rho_1} - \Lambda_i^{-1} \dot{\hat{\theta}}_i) \leq -L_i \hat{\theta}^T W_i$. Then, as a result,

$$\dot{\bar{V}}_2 \leq \sum_{i=m,s} \left(-\bar{k}_{i1} \|e_{i1}\|^{1+\rho_1} - \bar{k}_{i2} \|\xi_i\|^{1+\rho_1} - L_i \hat{\theta}^T W_i \right). \quad (25)$$

(1) For $t \in [0, \infty]$, with the defined W_i , the last term $L_i \hat{\theta}^T W_i$ can be ignored. Thus we have

$$\dot{V}_2 \leq \sum_{i=m,s} (-\bar{k}_{i1} \|e_{i1}\|^{1+\rho_1} - \bar{k}_{i2} \|\xi_i\|^{1+\rho_1}). \quad (26)$$

It is easy to derive that the variables e_{i1} , $\xi_i \in L_\infty \cap L_2$, and the system (16) is globally stable.

(2) For $t \in [T_e, \infty)$, applying the defined $W_i(t)$, one obtains

$$\begin{aligned} \dot{V}_2 &\leq \sum_{i=m,s} (-\bar{k}_{i1} \|e_{i1}\|^{1+\rho_1} - \bar{k}_{i2} \|\xi_i\|^{1+\rho_1} + \tilde{\theta}_i (Y_i^T(x_{i1}, x_{i2}) \mathcal{M}_{i0}^{-1}(x_{i1}) \xi_i^{2-\rho_1} + \Lambda_i^{-1} \tilde{\theta}_i)) \\ &\leq \sum_{i=m,s} \left(-\bar{k}_{i1} \|e_{i1}\|^{1+\rho_1} - \bar{k}_{i2} \|\xi_i\|^{1+\rho_1} - \frac{2^{\frac{\rho_1+1}{2}} \sigma_{ci}^{\rho_1} \lambda_{\min}(L_i)}{\lambda_{\max}(\Lambda_i^{-1})^{\frac{\rho_1+1}{2}}} \left(\frac{1}{2} \tilde{\theta}_i^T \Lambda_i^{-1} \tilde{\theta}_i \right)^{\frac{\rho_1+1}{2}} \right), \end{aligned} \quad (27)$$

which results in the boundedness of e_{i1} , ξ_i , $\tilde{\theta}_i$, and $\mathcal{F}_h + \mathcal{F}_e(t - T_s(t))$.

Then, let us choose

$$V_2 = V_1 + \sum_{i=m,s} \sum_{j=1}^n \int_{e_{i2j}^*}^{e_{i2j}} (s^{1/\rho_1} - e_{i2j}^{*/\rho_1})^{2-\rho_1} ds + \sum_{i=m,s} \frac{1}{2} \tilde{\theta}_i^T \Lambda_i^{-1} \tilde{\theta}_i. \quad (28)$$

Finally, one has

$$\begin{aligned} \dot{V}_2 &\leq -2^{\frac{\rho_1+1}{2}} \min(\bar{k}_{m1}, \bar{k}_{s1}) (V_1)^{\frac{\rho_1+1}{2}} - \left(\bar{k}_{m2} - \frac{1}{2} \right) 2^{-\frac{1-\rho_1^2}{2}} (2^{1-\rho_1} \xi_m^T \xi_m)^{\frac{\rho_1+1}{2}} - \bar{k}_{s2} 2^{-\frac{1-\rho_1^2}{2}} (2^{1-\rho_1} \xi_s^T \xi_s)^{\frac{\rho_1+1}{2}} \\ &\quad - \frac{2^{\frac{\rho_1+1}{2}} \sigma_{cm}^{\rho_1} \lambda_{\min}(L_m)}{\lambda_{\max}(\Lambda_m^{-1})^{\frac{\rho_1+1}{2}}} \left(\frac{1}{2} \tilde{\theta}_m^T \Lambda_m^{-1} \tilde{\theta}_m \right)^{\frac{\rho_1+1}{2}} - \frac{2^{\frac{\rho_1+1}{2}} \sigma_{cs}^{\rho_1} \lambda_{\min}(L_s)}{\lambda_{\max}(\Lambda_s^{-1})^{\frac{\rho_1+1}{2}}} \left(\frac{1}{2} \tilde{\theta}_s^T \Lambda_s^{-1} \tilde{\theta}_s \right)^{\frac{\rho_1+1}{2}} + \Psi \\ &\leq -\Omega V_2^{\frac{\rho_1+1}{2}} + \Psi, \end{aligned} \quad (29)$$

where $\Omega = \min(2^{\frac{\rho_1+1}{2}} \min(\bar{k}_{m1}, \bar{k}_{s1}), \bar{k}_{m2} 2^{-\frac{1-\rho_1^2}{2}}, \bar{k}_{s2} 2^{-\frac{1-\rho_1^2}{2}}, \frac{2^{\frac{\rho_1+1}{2}} \sigma_{cm}^{\rho_1} \lambda_{\min}(L_m)}{\lambda_{\max}(\Lambda_m^{-1})^{\frac{\rho_1+1}{2}}}, \frac{2^{\frac{\rho_1+1}{2}} \sigma_{cs}^{\rho_1} \lambda_{\min}(L_s)}{\lambda_{\max}(\Lambda_s^{-1})^{\frac{\rho_1+1}{2}}})$. $\Psi = 2 \|\mathcal{F}_h + \mathcal{F}_e(t - T_s(t))\|^2$.

Theorem 1. Consider the NNTSs described in (1) and the control algorithm (21). If there exist positive constants T_e , σ_{ci} , and T_d such that the IE condition $P(T_e) \geq \sigma_{ci}$ is satisfied, then we obtain the following.

(1) In free motion, i.e., $\mathcal{F}_h = \mathcal{F}_e = 0$, both the defined auxiliary system errors e_{i1} , e_{i2} and the system parameter learning errors $\tilde{\theta}_i$ will converge to zero in finite time. And the exact convergence time of the e_{i1} , e_{i2} , and $\tilde{\theta}_i$ is

$$T_c \leq \frac{2}{\Omega(1 - \rho_1)} V_2(0)^{\frac{1-\rho_1}{2}}. \quad (30)$$

(2) In other cases, all the defined auxiliary system errors e_{i1} , e_{i2} , the system parameter learning errors $\tilde{\theta}_i$, and the force synchronization error $\mathcal{F}_h + \mathcal{F}_e$ will converge to the neighborhood of zero in finite time.

Proof. In free motion, with the definitions for V_1 , V_2 , and the fact that $V_2 > 0$, $\dot{V}_2 \leq 0$, then we can obtain that e_{i1} , e_{i2} , $\tilde{\theta}_i \in L_\infty \cup L_2$. Moreover, with the inequality $\dot{V}_2 \leq -\Omega V_2^{\frac{\rho_1+1}{2}}$, it is obvious that e_{i1} , e_{i2} , and $\tilde{\theta}_i$ will converge to zero within t_1 . When the external forces are not zero, due to the term Ψ , with the inequality (29), it is evident that the defined auxiliary system errors e_{i1} , e_{i2} , the system parameter learning errors $\tilde{\theta}_i$, and the force synchronization error $\mathcal{F}_h + \mathcal{F}_e$ will converge in the neighborhood of zero in finite time, and the bound is related to the value of $\|\mathcal{F}_h + \mathcal{F}_e(t - T_s(t))\|$. This completes this proof.

Obviously, the finite-time convergence of $x_i - \psi_{i1}$, $\psi_{i1} = \psi_{i1} - \bar{x}_{i1}$ with $\bar{x}_{m1} = x_s(t - T_s(t))$, $\bar{x}_{s1} = x_m(t - T_m(t))$ will imply that $e_{i1} + \tilde{\psi}_{i1} = x_{i1} - \bar{x}_{i1}$ will converge to zero in finite time.

With the definitions for $\tilde{\psi}_{i1}$ and $\psi_{i1} = \psi_{i2}$, let us propose the following subsystem:

$$\dot{\tilde{\psi}}_{i1} = \psi_{i2} - \frac{d\bar{x}_{i1}}{dt}, \quad \dot{\psi}_{i2} = -k_{i4} \text{sig}(\zeta_i)^{\rho_4}, \quad (31)$$

where $\frac{d\bar{x}_{i1}}{dt}$ are the derivatives of \bar{x}_{i1} , $\zeta_i = \psi_{i2}^{1/\rho_3} - \psi_{i2}^{*/\rho_3}$ with the new auxiliary variables $\psi_{i2}^* = -k_{i3} \text{sig}(\psi_{i1})^{\rho_3}$, $k_{i3} \in \mathbb{R}_+$, $0 < \rho_3 < 1$, $k_{i4} \in \mathbb{R}_+$, and $0 < \rho_4 < 1$.

Proposition 1. The closed-loop NNTSs (1) are WFTIOS with the input vectors $\frac{d\bar{x}_{i1}}{dt}$ and the output vectors x_{i2} .

Proof. Choosing the Lyapunov function candidate as $U_1 = \sum_{i=m,s} \frac{1}{2} \tilde{\psi}_{i1}^T \tilde{\psi}_{i1}$, then one has

$$\dot{U}_1 = \sum_{i=m,s} \left(\tilde{\psi}_{i1}^T (\psi_{i2} - \psi_{i2}^*) - \tilde{\psi}_{i1}^T \frac{d\bar{x}_{i1}}{dt} - \tilde{\psi}_{i1}^T k_{i3} \text{sig}(\tilde{\psi}_{i1})^{\rho_3} \right). \quad (32)$$

Furthermore, let

$$U_2 = U_1 + \sum_{i=m,s} \sum_{j=1}^n \int_{\psi_{i2j}^*}^{\psi_{i2j}} (s^{1/\rho_3} - \psi_{i2j}^{*1/\rho_3})^{2-\rho_3} ds, \quad (33)$$

where ψ_{i2j} and ψ_{i2j}^* are the j th term of vectors ψ_{i2} and ψ_{i2}^* , respectively.

The derivative of U_2 is given as

$$\dot{U}_2 \leq \sum_{i=m,s} \left(-(k_{i3} - 1) \tilde{\psi}_{i1}^T \text{sig}(\tilde{\psi}_{i1})^{\rho_3} - \|\tilde{\psi}_{i1}\| \left\| \frac{d\bar{x}_{i1}}{dt} \right\| - (k_{i4} - \bar{c}_{i1} - \bar{c}_{i2}) \zeta_i^T \text{sig}(\zeta_i)^{\rho_3} + \bar{\Xi}_i \|\zeta_i\| \left\| \frac{d\bar{x}_{i1}}{dt} \right\| \right), \quad (34)$$

where $\bar{c}_{i1} = \frac{\rho_3 2^{(2-\rho_3)/\rho_3}}{(1+\rho_3)(1+\rho_3)/\rho_3}$, $\bar{c}_{i2} = \bar{\Xi}_i + \frac{(2\rho_3)^{\rho_3} (k_{i3} \bar{\Xi}_i)^{1+\rho_3}}{(1+\rho_3)^{1+\rho_3}}$ with $\bar{\Xi}_i = (2 - \rho_3) 2^{1-\rho_3} k_{i3}^{1/\rho_3}$. By setting $\rho_4 = 2\rho_3 - 1$, $k_{i3} - 1 - \bar{k}_{i3} = \eta_{i1}$, $k_{i4} - \bar{k}_{i4} - \bar{c}_{i1} - \bar{c}_{i2} = \eta_{i2}$ with $\bar{k}_{i3}, \bar{k}_{i4}, \eta_{i1}, \eta_{i2} \in \mathbb{R}_+$, it follows

$$\begin{aligned} \dot{U}_2 \leq \sum_{i=m,s} \left(-\eta_{i1} \tilde{\psi}_{i1}^T \text{sig}(\tilde{\psi}_{i1})^{\rho_3} - \eta_{i2} \zeta_i^T \text{sig}(\zeta_i)^{\rho_3} - \bar{k}_{i3} \tilde{\psi}_{i1}^T \text{sig}(\tilde{\psi}_{i1})^{\rho_3} \right. \\ \left. - \bar{k}_{i4} \zeta_i^T \text{sig}(\zeta_i)^{\rho_3} - \|\tilde{\psi}_{i1}\| \left\| \frac{d\bar{x}_{i1}}{dt} \right\| + \bar{\Xi}_i \|\zeta_i\| \left\| \frac{d\bar{x}_{i1}}{dt} \right\| \right). \end{aligned} \quad (35)$$

With the definition of U_2 , we know that $U_2 \leq \sum_{i=m,s} \frac{1}{2} \tilde{\psi}_{i1}^T \tilde{\psi}_{i1} + 2^{1-\rho_3} \zeta_i^T \zeta_i$; then there always exist two \mathcal{K}_∞ -functions ϕ_1, ϕ_2 , \mathcal{K} -functions ϕ_3, ϕ_4 such that

$$\phi_1(\|z(t)\|) \leq U_2 \leq \phi_2(\|z(t)\|), \quad (36)$$

where $z(t) = [\tilde{\psi}_{m1}^T, \tilde{\psi}_{s1}^T, \zeta_m^T, \zeta_s^T]^T$.

For any solution $z(t)$ and input $\frac{d\bar{x}_{i1}}{dt}$, it holds that

$$\|z(t)\| \geq \phi_4 \left(\left\| \frac{d\bar{x}_{i1}}{dt} \right\| \right) \Rightarrow \dot{U}_2 \leq \phi_3(\|z(t)\|), \quad (37)$$

where $\phi_3(\|z(t)\|) \sim U_2^{\frac{1+\rho_3}{2}}$.

With Definition 3, it is clear that $\tilde{\psi}_{i1}, \zeta_i$ are WFTISS with the inputs $\frac{d\bar{x}_{i1}}{dt}$ with the gains as $\phi_1^{-1} \circ \phi_2 \circ \phi_4$ (see Theorem 1 in [33] for details).

Furthermore, with $\|x_{i2}\| = \|e_{i2} - \psi_{i2}\| \leq \|e_{i2}\| + \|\zeta_i\|^{\rho_3} + k_{i3}^{\rho_3} \|\tilde{\psi}_{i1}\|^{\rho_3}$, then we can obtain that x_{i2} are WFTIOS with the input vectors $\frac{d\bar{x}_{i1}}{dt}$ for all $t > t_0$ and the fact that e_{i2} converges to zero in free motion in finite time. The corresponding gains are $\pi_i = (1 + k_{i3}^{\rho_3}) \phi_1^{-1} \circ \phi_2 \circ \phi_4$. This proof is completed.

Remark 2. In the above analysis, the \mathcal{K}_∞ -functions ϕ_1, ϕ_2 and \mathcal{K} -function ϕ_4 are easy to obtain. For example we just simply set $\phi_2(\|z(t)\|) = 2\|z(t)\|^2$ and $\phi_1(\|z(t)\|) = \frac{1}{2}\|z(t)\|^2$. Moreover, by setting $\|\tilde{\psi}_{i1}\| \geq (\frac{1}{k_{i3}} \|\frac{d\bar{x}_{i1}}{dt}\|)^{1/\rho_3}$, $\|\zeta_i\| \geq (\frac{\bar{\Xi}_i}{k_{i4}} \|\frac{d\bar{x}_{i1}}{dt}\|)^{1/\rho_3}$, it follows that $\phi_4(\|\frac{d\bar{x}_{i1}}{dt}\|) = ((\frac{1}{k_{i3}})^{1/\rho_3} + (\frac{\bar{\Xi}_i}{k_{i4}})^{1/\rho_3}) \|\frac{d\bar{x}_{i1}}{dt}\|^{1/\rho_3}$. Finally, the WFTISS gain can be achieved as $\pi_i = 4(1 + k_{i3}^{\rho_3})((\frac{1}{k_{i3}})^{1/\rho_3} + (\frac{\bar{\Xi}_i}{k_{i4}})^{1/\rho_3})$.

Based on Proposition 1, further one can have the following.

Theorem 2. The finite-time convergence of joint position error vectors $q_m - q_s(t - T_s(t))$, $q_s - q_m(t - T_m(t))$, $q_m - q_s$ and velocity vectors \dot{q}_m, \dot{q}_s will be ensured if the control gains k_{i3}, k_{i4} , and ρ_3 are chosen to satisfy $\pi_m(1 + \Upsilon_s) < 1$ and $\pi_s(1 + \Upsilon_m) < 1$.

Proof. According to the above analysis, consider the closed-loop teleoperation (1) with 2 input vectors and 2 output vectors, which can be ordered as $y_1 = x_{m2}, y_2 = x_{s2}, u_1 = \frac{d\bar{x}_{m1}}{dt}$, and $u_2 = \frac{d\bar{x}_{s1}}{dt}$.

Proposition 1 indicates that the NNTSs (1) are WFTIOS. Furthermore, the elements of the WFTIOS gain $\Gamma^0 = \{\gamma_{ij}^0\}$, $i = 1, 2, j = 1, 2$ with $\gamma_{11}^0 = \pi_m$, $\gamma_{12}^0 = 0$, $\gamma_{21}^0 = 0$, and $\gamma_{22}^0 = \pi_s$ can be determined.

Then, the estimations of the inputs $\frac{dx_i}{dt}$ can be obtained with Assumption 1 as follows:

$$\left| \frac{dx_{i1}(t - T_i(t))}{dt} \right| \leq (1 + \Upsilon_i) |x_{i2}(t - T_i(t))|. \quad (38)$$

Therefore, the interconnection elements are given as $\mathcal{M} := \{\mu_{ji}\}$, $i = 1, 2, j = 1, 2$ with $\mu_{11}^0 = 0$, $\mu_{12}^0 = 1 + \Upsilon_s$, $\mu_{21}^0 = 1 + \Upsilon_m$, $\mu_{22}^0 = 0$.

According to the above expressions, it is concluded that the closed-loop gain elements are given by $\pi_m(1 + \Upsilon_s)$ and $\pi_s(1 + \Upsilon_m)$. Applying Lemma 1, by choosing controller gains to make inequalities $\pi_m(1 + \Upsilon_s) < 1$ and $\pi_s(1 + \Upsilon_m) < 1$ hold, then we can conclude that all $\tilde{\psi}_{i1}$, ψ_{i2} , $x_{i2} \in L_\infty$ and $\tilde{\psi}_{i1} \rightarrow 0$, $\psi_{i2} \rightarrow 0$, $x_{i2} \rightarrow 0$ in finite time.

Thus with the definitions for $\tilde{\psi}_{i1}$, ψ_{i2} , e_{i1} , and e_{i2} , we can directly obtain the finite-time convergence of $x_{i1} - \bar{x}_{i1}$ and x_{i2} . Furthermore, with $q_m - q_s(t - T_s(t)) = q_m - q_s + q_s - q_s(t - T_s(t)) = q_m - q_s + \int_{t-T_s(t)}^t \dot{q}_s(\delta) d\delta$, it is obvious that the finite-time convergence of $q_m - q_s$ can also be achieved directly. The proof for Theorem 2 is completed.

Remark 3. In general cases, the force/position hybrid control and the impedance control are applied to improve the transparency of NNTSs. Compared with the impedance control which is more sensitive to system uncertainties [38], the force/position hybrid control is more suitable for uncertain NNTSs. Meanwhile, to avoid the increase of system energy caused by direct transmission force, the virtual force transmission method proposed in [39, 40] can be applied.

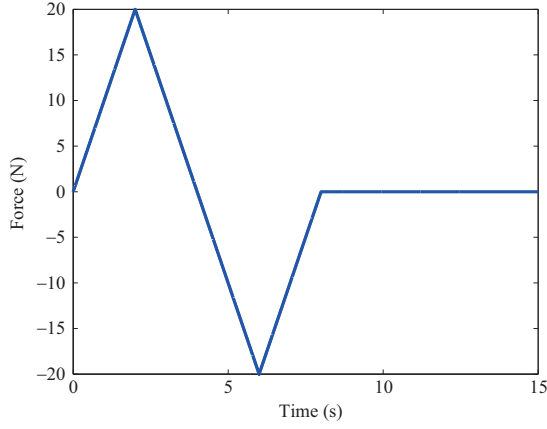
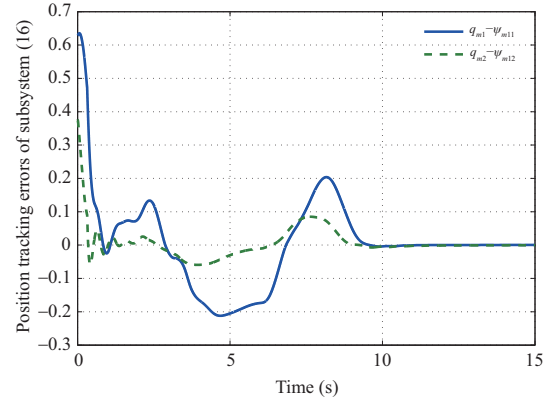
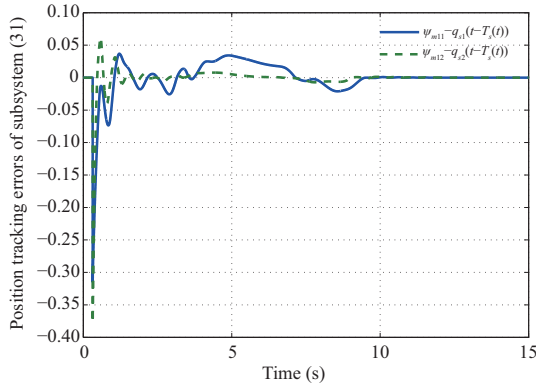
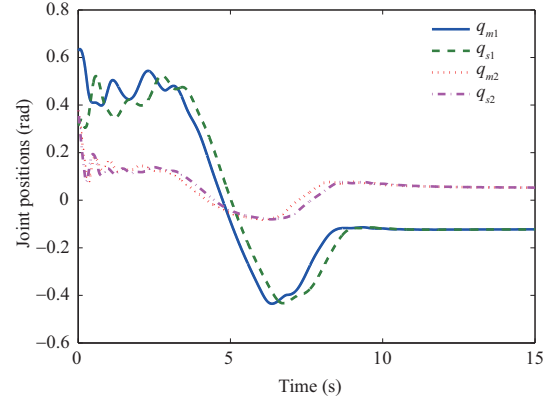
Remark 4. In recent years, intelligent learning techniques such as NNs and FLs have been widely used for estimation of system uncertainties. Yet, the complexity of neural weight or fuzzy rule training makes the practical application of intelligent learning techniques problematic. Parameter adaptive estimation method provides an alternative method for system uncertainties estimation. However, the traditional parameter estimation law can only ensure the boundedness of the parameter estimation error. To tackle this issue, the exact parameter estimation result is achieved in [29, 30] under the PE condition, which is difficult to guarantee in practice [26, 27]. Compared with the PE condition, the IE condition can alleviate the requirement, which only needs to be maintained for an interval. According to this observation, the adaptive finite-time parameter estimation problem under the IE condition is addressed in this paper. Firstly, not only the system synchronization errors but also the parameter learning errors are employed to drive the new parameter update laws. Secondly, besides the system parameter online instantaneous data, the parameter historical data are explored to make parameter error convergence under a more realizable IE condition. Moreover, different from [26] an adjustable forgetting factor is applied to trade off the effect of the historical data and the instantaneous data. Then better parameter estimation will be achieved.

Remark 5. In this paper, the finite-time force and position synchronization control is fulfilled. It is well known, based on the finite-time control theory, the derived system convergence time depends on the initial states of the system. The fixed-time control [40] and predefined-time control [41] are introduced and then developed by many authors. It is worth noting that based on the theoretical innovation achieved in this paper, it is not difficult to ensure the fixed-time and predefined-time stability for the NNTSs by adding high power terms to the controller and parameter adaptive law.

4 Simulation and experiment

4.1 Simulation validations

In this subsection, two identical 2-DOF manipulators are chosen to constitute the master-slave teleoperation system [4]. For simulation, the actual parameters of system model are set as $m_1 = 0.5$ kg, $m_2 = 1$ kg, $l_1 = 1$ m, $l_2 = 0.8$ m, and $g = 9.81$ m/s². The joint mass uncertainties are considered for the slave manipulator by assuming that we can obtain $m_{1o} = 0.39$ kg, $m_{2o} = 0.846$ kg, $l_{1o} = 1$ m, $l_{2o} = 0.8$ m in reality. The communication time delays between the local side and the remote side are set as $T_m(t) = 200 + 100\sin(t)$ ms and $T_s(t) = 260 + 100\sin(t)$ ms. In simulation, set the controller parameters as $k_{m1} = k_{s1} = \text{diag}(6, 6)$, $k_{m2} = k_{s2} = \text{diag}(6, 6)$, $k_{m3} = k_{s3} = \text{diag}(1, 1)$, $k_{m4} = k_{s4} = \text{diag}(10, 10)$ with


Figure 1 (Color online) Human operator insert force F .

Figure 2 (Color online) Position tracking errors e_{m1} of subsystem (16).

Figure 3 (Color online) Position tracking errors $\tilde{\psi}_{m1}$ of subsystem (31).

Figure 4 (Color online) Joint positions of the master and the slave.

$\rho_1 = \rho_3 = 9/11$, $\rho_2 = \rho_4 = 7/11$, $\Lambda_s = \text{diag}(1, 1)$, $L_s = \text{diag}(0.1, 0.1)$. The initial values of joint position and velocity for the master and the slave are set as $q_m(0) = [0.2\pi \ 0.12\pi]^T$, $q_s(0) = [0.1\pi \ 0.12\pi]^T$, $\dot{q}_m(0) = \dot{q}_s(0) = [0 \ 0]^T$. It is evident that under the chosen controller parameters, the conditions $\pi_m(1 + \Upsilon_s) < 1$ and $\pi_s(1 + \Upsilon_m) < 1$ hold. A human force F in the Y direction shown in Figure 1 is applied to the master site. As we can see in Figure 1, the human operator inserted force is 0 at 0 s, grows to 20 N at 2 s, and goes down to zero from 2 to 4 s. Then the force decreases to -20 N from 4 to 6 s and increases to zero at 8 s. With the human-force input, we know that the torque $F_h = J_m^T \times [0 \ 1]^T \times F$, then the torque $F_e = J_s^T \times [0 \ 1]^T \times 120000N \times (y - 0.4)$. Furthermore, the corresponding simulation results are presented in Figures 1–8. In Figures 2 and 3, the trajectories of variables $e_{m1} = [q_{m1} - \psi_{m11}; q_{m2} - \psi_{m12}]$ and $\tilde{\psi}_{m1} = [\psi_{m11} - q_{s1}(t - T_s(t)); \psi_{m12} - q_{s2}(t - T_s(t))]$ are shown for two joints, respectively. In Figure 4, the synchronization errors $q_m - q_s$ are given, respectively. It is evident that the finite-time position synchronization performance can be achieved based on Figures 2–4. Furthermore, to verify the parameters composite learning ability, the estimations for the unknown parameters $m_1 - m_{1o}$ and $m_2 - m_{2o}$ are shown in Figure 5. Obviously, the unknown system mass parameters can be precisely estimated in finite time. The control torques of master $\tau_m = [\tau_{m1}; \tau_{m2}]$ and slave $\tau_s = [\tau_{s1}; \tau_{s2}]$ for joints 1 and 2 are shown in Figure 6. The superior torque reflecting the property of the teleoperation system in the case of crash is shown in Figure 7. It can be seen that when the slave hit the wall at 1 s, a large environmental force was instantly generated. Figure 8 presents that the slave robot is stuck at the position of 0.4 m at 1 s and begins to move in reverse at 4.8 s. Then, due to the application of human force in the negative direction, the slave gradually moved away from the wall in reverse motion with the environmental torques gradually decreasing. In the end, the effectiveness and the fast and precise synchronization performance

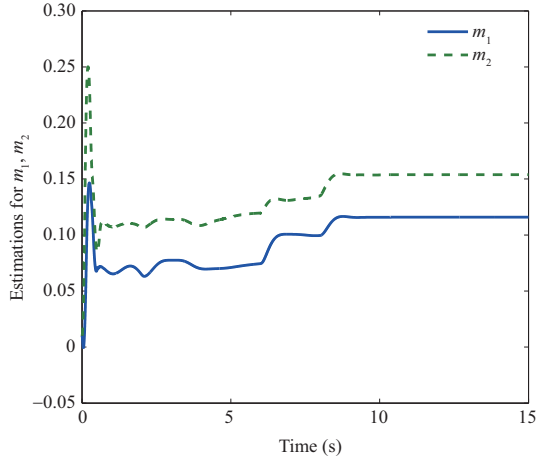


Figure 5 (Color online) Estimations for the unknown m_1 and m_2 .

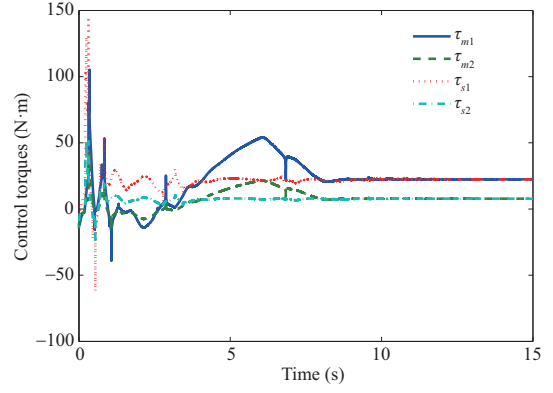


Figure 6 (Color online) Control torques for the master and the slave.

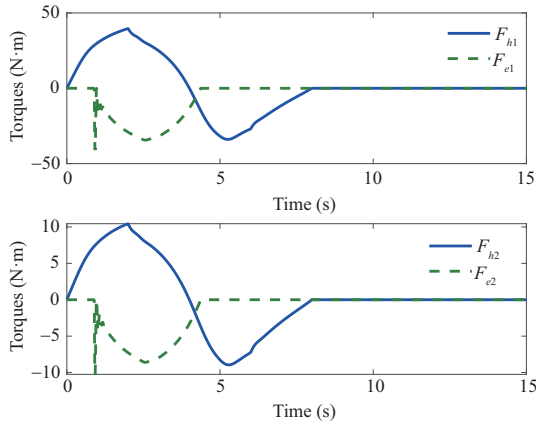


Figure 7 (Color online) Torques of the human and external environments.

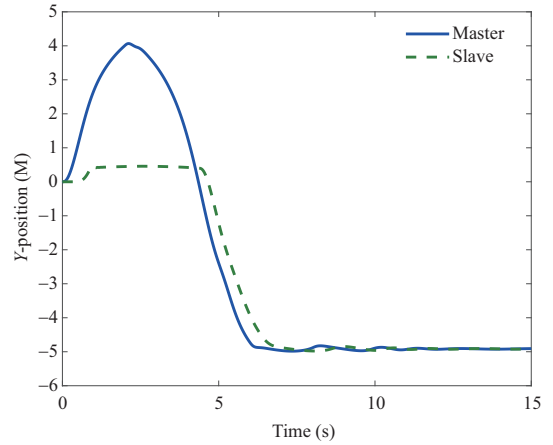


Figure 8 (Color online) Y-position of the master and slave.

of the developed control algorithm have been verified through the above simulation results.

4.2 Experimental validations

In addition to simulation results, hardware experimental results will also be provided to further validate the effectiveness and robustness of the proposed CLFTAC approach. The 3-DOF NNTS platform consisting of two Phantom Premium 1.5A robots (SensAble Technologies, Inc.) is shown in Figure 9 (for a detailed introduction for our platform, please refer to our previous literature [7]). In the experiment, because the exact system parameters of the platform are totally unknown, we choose $\mathcal{M}_{io}(q_i) = \text{diag}(0.2)$. Parameter adaptive method is applied to estimate unknown $F_i(q_i, \dot{q}_i, \ddot{q}_i) = (M_i(q_i) - M_{io}(q_i))\ddot{q}_i + C_i(q_i, \dot{q}_i)\dot{q}_i + G_i(q_i)$. Furthermore, parameters of the designed controller are selected as $k_{m1} = k_{s1} = \text{diag}(0.2, 0.5, 0.6)$, $k_{m2} = k_{s2} = \text{diag}(0.2, 0.3, 0.4)$, $k_{m3} = k_{s3} = \text{diag}(0.1, 0.1, 0.1)$, $k_{m4} = k_{s4} = \text{diag}(1, 1, 1)$ with $\rho_1 = \rho_3 = 9/11$, $\rho_2 = \rho_4 = 7/11$, $\Lambda_s = \text{diag}(1, 1, 1)$, and $L_s = \text{diag}(0.1, 0.1, 0.1)$.

4.2.1 Effectiveness validations under different time delays

The time delay of three cases will be considered. Case 1: $T_m(t) = T_s(t) = 50 + 40\sin(t)$ ms; Case 2: $T_m(t) = T_s(t) = 100 + 60\sin(t)$ ms; Case 3: the random jittering delay signals. The corresponding master-slave position tracking results are shown in Figure 10 for three joints, respectively. According to Figure 10, it can be stated that when the operator holds the master robot to make it move, due to the



Figure 9 (Color online) Experimental platform of networked teleoperation systems.

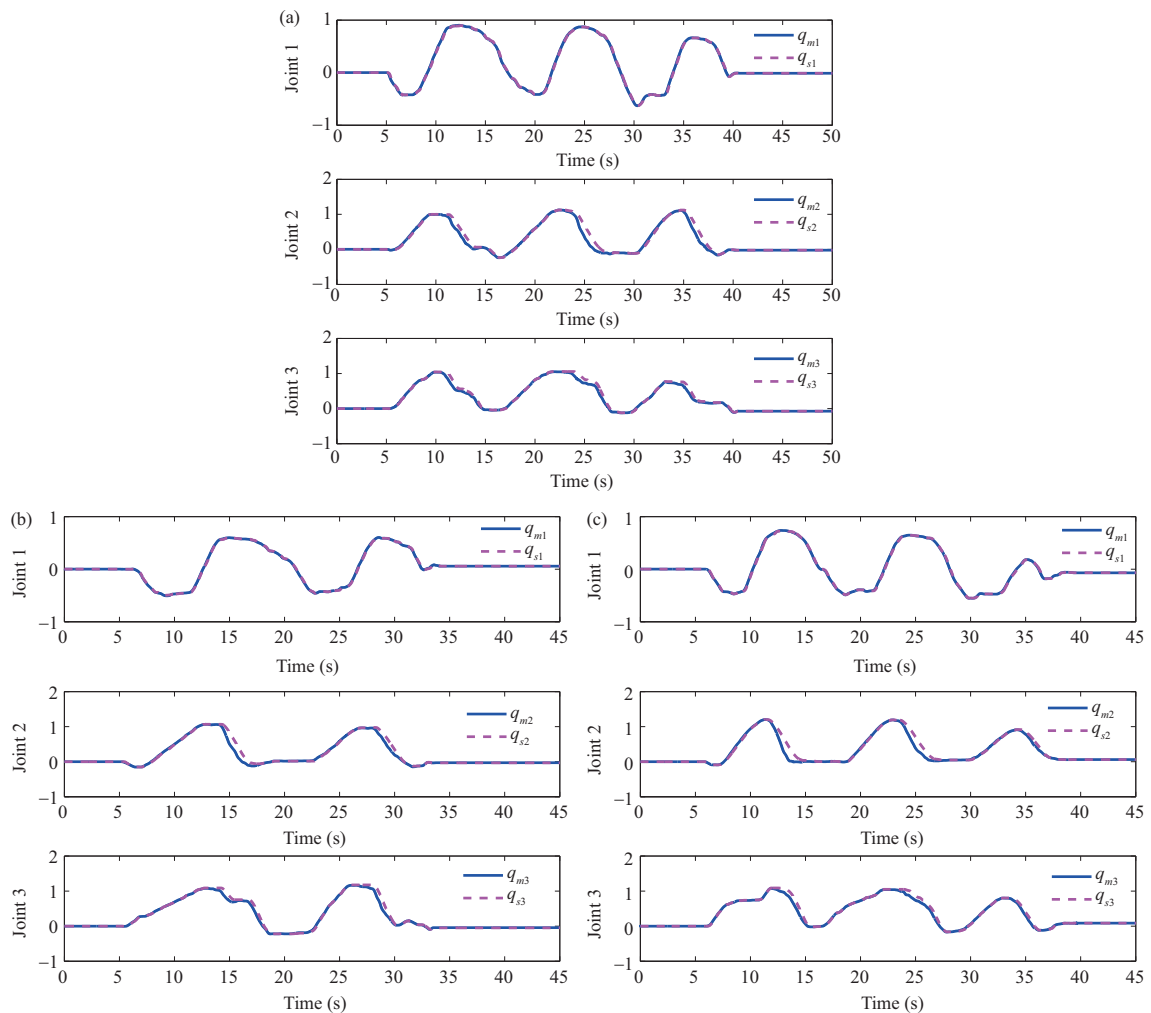


Figure 10 (Color online) Trajectories of the master and slave during free motion under (a) $T_m(t) = T_s(t) = 50 + 40\sin(t)$ ms, (b) $T_m(t) = T_s(t) = 100 + 60\sin(t)$ ms, and (c) random jittering time-varying delays.

proposed controller, the slave robot will follow the master robot to move accordingly. Yet, owing to a delay in network communication channels, there are position synchronization errors between the master and slave, and the size of the tracking errors varies with different time-varying delays. Meanwhile, it is also evident that in free motion, the position synchronization errors $q_m - q_s$ will rapidly converge to zero. Figure 11 shows the relevant torque reflecting properties in the X -direction and Y -direction, respectively, in which it can be seen that the environment torque fluctuates around zero due to slave's no collision

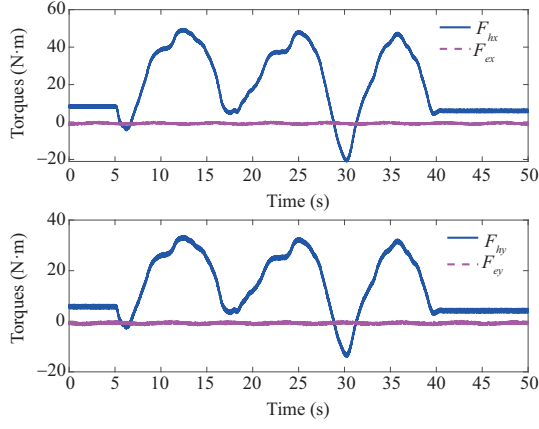


Figure 11 (Color online) Torques of the master and slave under $T_m(t) = T_s(t) = 100 + 60\sin(t)$ ms.

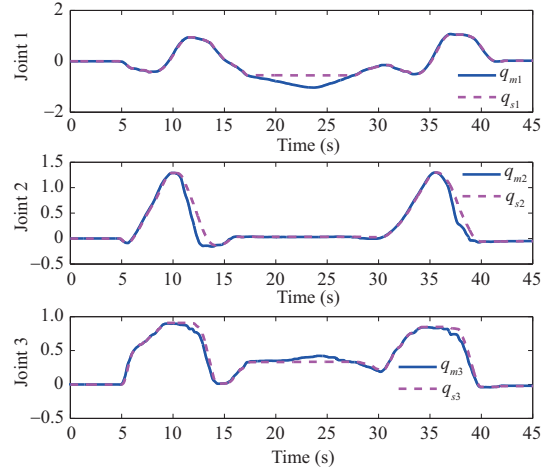


Figure 12 (Color online) Trajectories of the master and slave during contact under $T_m(t) = T_s(t) = 100 + 60\sin(t)$ ms.

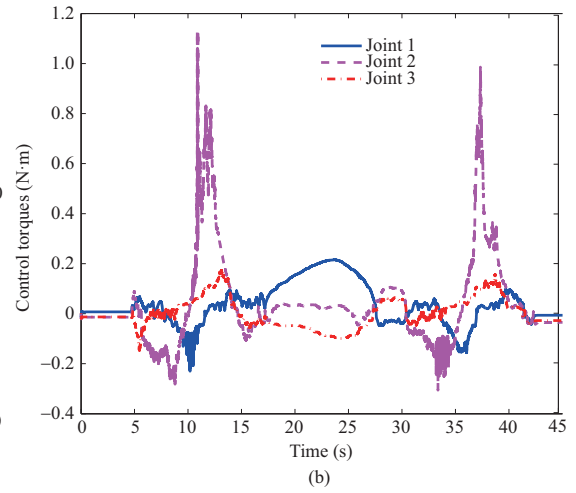
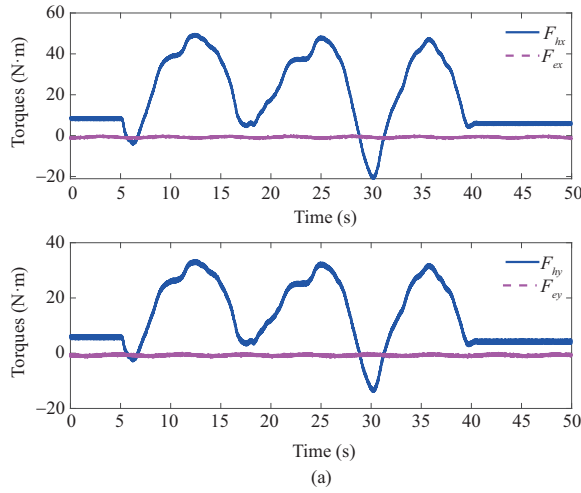


Figure 13 (Color online) (a) Torques of the human and external environments in Case 2; (b) control torques of the slave under $T_m(t) = T_s(t) = 100 + 60\sin(t)$ ms.

with the external environment.

4.2.2 Effectiveness validations when contacting with an object

Furthermore, we will verify the validity of the proposed control approach in the case of a collision between a slave robot and an object under time delays $T_m(t) = T_s(t) = 100 + 60\sin(t)$ ms. In the experiment, we place an object next to the slave robot, and the slave robot will close to the object by tracking the path of the master robot, which is manipulated by the human operator. Eventually, the slave robot will contact the object. At this point, if the operator continues to push the master robot, the operator will feel more and more resistance. In order not to damage the slave robot and object, the operator moves the end of the master robot in the opposite direction. At this point, due to the change of the master robot's trajectory, the slave robot will adjust its trajectory under the action of the controller and continue to follow the master robot's movement, while slowly leaving the object. When the master robot stops moving, the master-slave synchronization error rapidly approaches zero. The relevant experimental results can be seen in Figures 12–14. In Figure 12, we can see that when the movement direction of the master robot changes suddenly and the collision occurs between the slave robot and the object, the master-slave synchronization error will be relatively large due to the effect of time delay, but satisfactory synchronization performance can be obtained in the rest period. Figure 13(a) depicts the torque reflecting property in the X-direction and Y-direction for the master and the slave, respectively. It is clear that

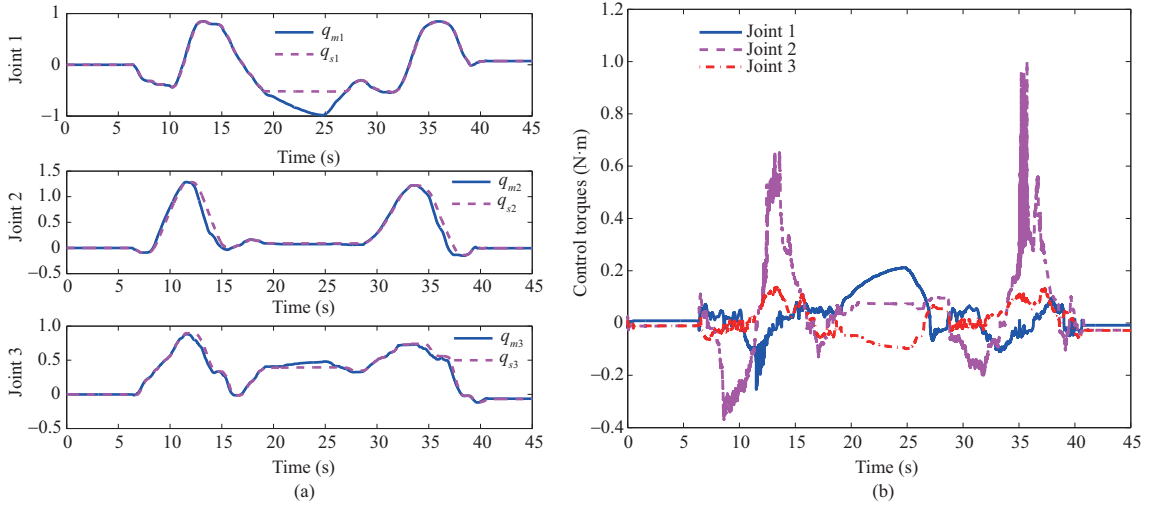


Figure 14 (Color online) Trajectories of the master and slave (a) and control torques of the slave (b) under random jittering delay signals.

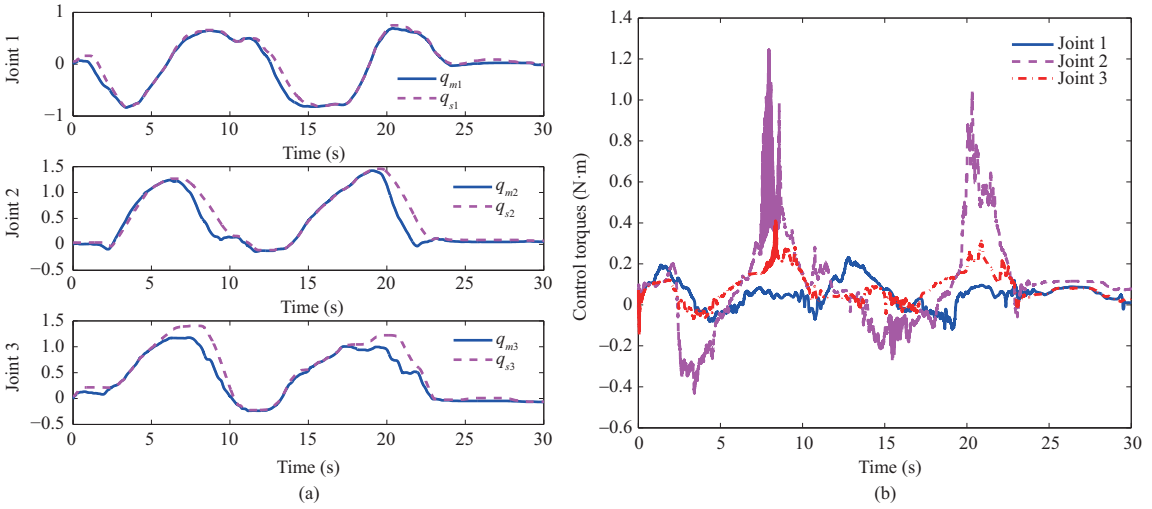


Figure 15 (Color online) Trajectories of the master and slave (a) and control torques of the slave (b) under random jittering delay signals with unknown external disturbances.

when the operator moves the master robot, the force exerted by the operator increases, and the force exerted by the environment increases suddenly only when the slave robot collides with an external object. Figure 13(a) presents that the slave robot is stuck at the position of -0.5 m at 17 s and begins to move in reverse at 27 s. Then, due to the application of human force in the opposite direction, the environmental force gradually tends to zero. Figure 13(b) shows that the control torque of the slave robot is always bounded and varies with the synchronization error of the master-slave robot. Similarly, the random jittering delay is also considered and corresponding experimental results are shown in Figures 14(a) and (b). It is evident that, satisfactory master-slave synchronization performance can also be guaranteed even under the random jittering delay.

4.2.3 Effectiveness validations of system robustness

Finally, the robustness of the proposed control algorithm is further verified in the presence of unknown external disturbances $d(t) = 0.1 + 0.06\sin(t)$ and random jittering time-varying delays. In Figure 15(a), the position trajectories of the master and slave are given. Obviously, satisfactory position synchronization performance can also be obtained even if there exist unknown external disturbances in experiments. Additionally, Figure 15(b) depicts the slave robot's control torques. It can be seen that the control torque of the slave robot is always bounded, that is, the system always runs stably.

5 Conclusion

In this article, the delay-dependent finite-time synchronization performance is achieved for a class of NNTSs with asymmetric time-varying delays in the presence of system uncertainties. A new robust CLFTAC approach is designed to make the position synchronization errors and the parameter learning errors simultaneously converge to zero in finite time. Thus, the robustness of the closed-loop NNTSs is enhanced greatly. This paper provides the first composite learning finite-time control results for NNTSs under such weak conditions as communication time-delays and system excitation conditions. Furthermore, the finite-time stability of the closed-loop system is proven by proposing the proper Lyapunov function and multi-dimension finite-time small-gain theorem, strictly. Finally, the superior performance of the designed control strategy is verified with the simulation and experimental results. In the future, the fresh and powerful approaches such as the deep reinforcement learning strategy [42] and the event-triggered control method [43] will be considered in teleoperation systems NNTSs to obtain better synchronization performance.

Acknowledgements This work was supported in part by National Natural Science Foundation of China (Grant Nos. 62373319, 61933009, 62073276), Natural Science Foundation of Hebei Province (Grant Nos. F2022203036, F2021203109, F2021203054, F2022203025), and Provincial Key Laboratory Performance Subsidy Project (Grant No. 22567612H).

References

- Hokayem P F, Spong M W. Bilateral teleoperation: an historical survey. *Automatica*, 2006, 42: 2035–2057
- Zhang B, Li H Y, Tang G J. Human control model in teleoperation rendezvous. *Sci China Inf Sci*, 2014, 57: 112205
- Kebria P M, Khosravi A, Nahavandi S, et al. Robust adaptive control scheme for teleoperation systems with delay and uncertainties. *IEEE Trans Cybern*, 2020, 50: 3243–3253
- Zhao Z H, Yang J, Liu C J, et al. Nonlinear composite bilateral control framework for n-DOF teleoperation systems with disturbances. *Sci China Inf Sci*, 2018, 61: 070221
- Hua C C, Liu X P. Delay-dependent stability criteria of teleoperation systems with asymmetric time-varying delays. *IEEE Trans Robot*, 2010, 26: 925–932
- Yang Y N, Yan Y W, Hua C C, et al. Prescribed performance control for teleoperation system of nonholonomic constrained mobile manipulator without any approximation function. *IEEE Trans Automat Sci Eng*, 2023. 1–12
- Baranitha R, Mohajerpoor R, Rakkiyappan R. Bilateral teleoperation of single-master multislave systems with semi-markovian jump stochastic interval time-varying delayed communication channels. *IEEE Trans Cybern*, 2021, 51: 247–257
- Dong S L, Chen G R, Liu M Q, et al. Cooperative neural-adaptive fault-tolerant output regulation for heterogeneous nonlinear uncertain multiagent systems with disturbance. *Sci China Inf Sci*, 2021, 64: 172212
- Zhao L, Yu J P, Wang Q G. Adaptive finite-time containment control of uncertain multiple manipulator systems. *IEEE Trans Cybern*, 2022, 52: 556–567
- Zhu Y P, Zhu W Y, Liu J P, et al. Command-filtered finite-time fuzzy adaptive fault-tolerant control of output-constrained robotic manipulators with unknown dead-zones. *IEEE Trans Circuits Syst II*, 2023, 70: 2939–2943
- Yang Y N, Hua C C, Guan X P. Adaptive fuzzy finite-time coordination control for networked nonlinear bilateral teleoperation system. *IEEE Trans Fuzzy Syst*, 2014, 22: 631–641
- Yang Y N, Hua C C, Guan X P. Finite time control design for bilateral teleoperation system with position synchronization error constrained. *IEEE Trans Cybern*, 2016, 46: 609–619
- Wang J W, Tian J W, Zhang X, et al. Control of time delay force feedback teleoperation system with finite time convergence. *Front Neurobot*, 2022. doi: 10.3389/fnbot.2022.877069
- Zhai D H, Xia Y Q. Finite-time control of teleoperation systems with input saturation and varying time delays. *IEEE Trans Syst Man Cybern Syst*, 2017, 47: 1522–1534
- Wang Z W, Liang B, Sun Y C, et al. Adaptive fault-tolerant prescribed-time control for teleoperation systems with position error constraints. *IEEE Trans Ind Inf*, 2020, 16: 4889–4899
- Zhang H C, Song A G, Li H J, et al. Novel adaptive finite-time control of teleoperation system with time-varying delays and input saturation. *IEEE Trans Cybern*, 2021, 51: 3724–3737
- Bao J L, Wang H Q, Liu P X. Finite-time synchronization control for bilateral teleoperation systems with asymmetric time-varying delay and input dead zone. *IEEE ASME Trans Mechatron*, 2021, 26: 1570–1580
- Yang Y N, Hua C C, Li J P. A novel delay-dependent finite-time control of telerobotics system with asymmetric time-varying delays. *IEEE Trans Contr Syst Technol*, 2022, 30: 985–996
- Zhang H C, Song A G, Li H J, et al. Adaptive finite-time control scheme for teleoperation with time-varying delay and uncertainties. *IEEE Trans Syst Man Cybern Syst*, 2022, 52: 1552–1566
- Li L N, Liu Z X, Ma Z Q, et al. Adaptive neural learning finite-time control for uncertain teleoperation system with output constraints. *J Intell Robot Syst*, 2022, 105: 1–16
- Yang Y N, Hua C C, Li J P, et al. Finite-time output-feedback synchronization control for bilateral teleoperation system via neural networks. *Inf Sci*, 2017, 406–407: 216–233
- Yang Y N, Jiang H X, Gan L, et al. Fixed-time composite neural learning control of flexible telerobotic systems. *IEEE Trans Cybern*, 2023
- Yang Y N, Jiang H C, Hua C C, et al. Practical preassigned fixed-time fuzzy control for teleoperation system under scheduled shared-control framework. *IEEE Trans Fuzzy Syst*, 2023. 1–12
- Pan Y P, Yu H Y. Composite learning robot control with guaranteed parameter convergence. *Automatica*, 2018, 89: 398–406
- Yang Y N, Hua C C, Li J P. Composite adaptive guaranteed performances synchronization control for bilateral teleoperation system with asymmetrical time-varying delays. *IEEE Trans Cybern*, 2022, 52: 5486–5497
- Na J, Xing Y S, Costa-Castello R. Adaptive estimation of time-varying parameters with application to roto-magnet plant. *IEEE Trans Syst Man Cybern Syst*, 2021, 51: 731–741

- 27 Li Y L, Yin Y X, Zhang S, et al. Composite adaptive control for bilateral teleoperation systems without persistency of excitation. *J Franklin Institute*, 2020, 357: 773–795
- 28 Na J, Mahyuddin M N, Herrmann G, et al. Robust adaptive finite-time parameter estimation and control for robotic systems. *Intl J Robust Nonlinear*, 2020, 25: 3045–3071
- 29 Yang C G, Jiang Y M, He W, et al. Adaptive parameter estimation and control design for robot manipulators with finite-time convergence. *IEEE Trans Ind Electron*, 2018, 65: 8112–8123
- 30 Zhang Y, Hua C C. Composite learning finite-time control of robotic systems with output constraints. *IEEE Trans Ind Electron*, 2023, 70: 1687–1695
- 31 Makkar C, Hu G, Sawyer W G, et al. Lyapunov-based tracking control in the presence of uncertain nonlinear parameterizable friction. *IEEE Trans Automat Contr*, 2007, 52: 1988–1994
- 32 Bhat S P, Bernstein D S. Finite-time stability of continuous autonomous systems. *SIAM J Control Optim*, 2000, 38: 751–766
- 33 Abdessameud A, Polushin I G, Tayebi A. Synchronization of lagrangian systems with irregular communication delays. *IEEE Trans Automat Contr*, 2014, 59: 187–193
- 34 Hong Y G, Jiang Z P, Feng G. Finite-time input-to-state stability and applications to finite-time control design. *SIAM J Control Optim*, 2010, 48: 4395–4418
- 35 Hong Y G, Wang J K, Cheng D Z. Adaptive finite-time control of nonlinear systems with parametric uncertainty. *IEEE Trans Automat Contr*, 2006, 51: 858–862
- 36 Huang X Q, Lin W, Yang B. Global finite-time stabilization of a class of uncertain nonlinear systems. *Automatica*, 2018, 41: 881–888
- 37 Sanchez E, Alanis A. Adaptive approximation based control: unifying neural, fuzzy and traditional adaptive approximation approaches (Farrell J A, Polycarpou M M [Book review]). *IEEE Trans Neural Netw*, 2008, 19: 731–732
- 38 Shen H H, Pan Y J. Improving tracking performance of nonlinear uncertain bilateral teleoperation systems with time-varying delays and disturbances. *IEEE ASME Trans Mechatron*, 2020, 25: 1171–1181
- 39 Chen Z, Huang F H, Sun W C, et al. RBF-neural-network-based adaptive robust control for nonlinear bilateral teleoperation manipulators with uncertainty and time delay. *IEEE ASME Trans Mechatron*, 2020, 25: 906–918
- 40 Zhang S, Yuan S, Yu X B, et al. Adaptive neural network fixed-time control design for bilateral teleoperation with time delay. *IEEE Trans Cybern*, 2022, 52: 9756–9769
- 41 Xu J Z, Ge M F, Ling G, et al. Hierarchical predefined-time control of teleoperation systems with state and communication constraints. *Intl J Robust Nonlinear*, 2021, 31: 9652–9675
- 42 Bacha S C, Bai W B, Wang Z W, et al. Deep reinforcement learning-based control framework for multilateral telesurgery. *IEEE Trans Med Robot Bion*, 2022, 4: 352–355
- 43 Wang Z W, Lam H K, Guo Y, et al. Adaptive event-triggered control for nonlinear systems with asymmetric state constraints: a prescribed-time approach. *IEEE Trans Automat Contr*, 2023, 68: 3625–3632

Appendix A Proof of Lemma 1

\mathbb{R}_+^n denotes the positive orthant in \mathbb{R}^n , i.e., $\mathbb{R}_+^n := \{(\eta_1, \eta_2, \dots, \eta_n)^T \in \mathbb{R}^n, \text{ s.t. } \eta_i \geq 0 \forall i = 1, \dots, n\}$. Let $\|Y\| := (\|y_1\|, \|y_2\|, \dots, \|y_q\|)^T \in \mathbb{R}_+^q$ and $\beta(\|\eta\|, t) := [\beta_1(\|\eta\|, t), \beta_2(\|\eta\|, t), \dots, \beta_q(\|\eta\|, t)]^T \in \mathbb{R}_+^q$, where $\beta_i \in \mathcal{GKL}$ are the functions from the definition of WFTIOS (Definition 2).

First of all, note that $u_j(t) \equiv 0$ for $t < 0$ implies that $\eta(t)$ is well-defined for $t \leq 0$. Also, the WFTIOS property implies that

$$\sup_{t \in [-T^*(0), 0]} \|Y\| \leq \beta(\|\eta(-T^*(0))\|, -T^*(0)). \quad (\text{A1})$$

According to the inequality (11) and the local Lipschitzness of $h_i(x)$, the solution of systems (9), (11) exists at least for all $t < t^*$, where $t^* > 0$. Because of the assumptions presented in this paper, one has

$$\begin{aligned} \sup_{t \in [0, t^*]} \|Y\| &\leq \beta(\|\eta(0)\|, t) + \Gamma \cdot \sup_{t \in [-T^*(0), t^*]} \|Y\| \\ &\leq \beta(\|\eta(0)\|, t) + \Gamma \cdot \left(\sup_{t \in [-T^*(0), 0]} \|Y\| + \sup_{t \in [0, t^*]} \|Y\| \right) \\ &\leq \beta(\|\eta(0)\|, t) + \Gamma \cdot \left(\beta(\|x(-T^*(0))\|, -T^*(0)) + \sup_{t \in [0, t^*]} \|Y\| \right). \end{aligned} \quad (\text{A2})$$

These inequalities imply

$$[I - \Gamma] \cdot \sup_{t \in [0, t^*]} \|Y\| \leq \beta(\|\eta(0)\|, t) + \Gamma \cdot \beta(\|\eta(-T^*(0))\|, -T^*(0)), \quad (\text{A3})$$

where I denotes the unit matrix with corresponding dimensions. As we all know, for a matrix $\Gamma \in \mathbb{R}^{q \times q}$ with all nonnegative elements, the inequality $\rho(\Gamma) < 1$ implies that the matrix $[I - \Gamma]$ is invertible and all elements of the matrix $[I - \Gamma]^{-1}$ are nonnegative. Therefore, we have

$$\sup_{t \in [0, t^*]} \|Y\| \leq [I - \Gamma]^{-1} \left(\begin{array}{c} \beta(\|\eta(0)\|, t) \\ + \Gamma \cdot \beta(\|\eta(-T^*(0))\|, -T^*(0)) \end{array} \right). \quad (\text{A4})$$

And when $t^* \geq T(r)$, we have $\sup_{t \in [0, t^*]} \|Y\| \leq [I - \Gamma]^{-1} \Gamma \cdot \beta(\|x(-T^*(0))\|, -T^*(0))$, and it is easy to see that $t^* = +\infty$.

The uniform boundedness of $y_i(t)$, $i \in \mathcal{N}_q$ $y_i(t)$, $i \in \mathcal{N}_q$, therefore, is proven. The uniform boundedness of $u_j(t)$, $j \in \mathcal{N}_p$, now follows directly from (9) and (11).

To prove the finite-time convergence, note that

$$\lim_{t \rightarrow T(r)} \|Y(t)\| \leq \Gamma \lim_{t \rightarrow T(r)} \left(\sup_{s \in [t - T^*(t), t]} \|Y(s)\| \right). \quad (\text{A5})$$

Due to Assumption 1, one has

$$\lim_{t \rightarrow T(r)} \left(\sup_{s \in [t-T^*(t), t]} \|Y(s)\| \right) = \limsup_{t \rightarrow T(r)} \|Y(t)\|, \quad (\text{A6})$$

and therefore we have

$$[1 - \Gamma] \cdot \limsup_{t \rightarrow T(r)} \|Y(t)\| \leq 0. \quad (\text{A7})$$

Since $[1 - \Gamma]$ has full rank, the above inequality implies $\limsup_{t \rightarrow T(r)} \|Y(t)\| = 0$. This proves the convergence $y_i(t)$, $i \in \mathcal{N}_q$, and the convergence of $u_j(t)$, $j \in \mathcal{N}_p$, following from (11) and Assumption 1. It is completed.

Appendix B Auxiliary filters design

The auxiliary filters addressed in this paper are as follows. According to Property 2, a linearly parameterized master-slave NNTS model can be obtained as

$$\tau_i - Y_i(x_{i1}, x_{i2}, \dot{x}_{i2})\Theta_i + F_{ihe} = Y_i(x_{i1}, x_{i2}, \dot{x}_{i2})\theta_i, \quad (\text{B1})$$

where $M_{io}(q_i)\ddot{q}_i + C_{io}(q_i, \dot{q}_i)\dot{q}_i + G_{io}(q_i) = Y_i(x_{i1}, x_{i2}, \dot{x}_{i2})\Theta_i$.

By applying the designed nonlinear filter, it is easy to have $Y_{if}(x_{i1}, x_{i2}, \dot{x}_{i2})\theta_i = \tau_{if} - Y_{if}(x_{i1}, x_{i2}, \dot{x}_{i2})\Theta_i + F_{ihef}$. After passing through the filter, $Y_i(x_{i1}, x_{i2}, \dot{x}_{i2})$, τ_i , and F_{ihe} are represented as $Y_{if}(x_{i1}, x_{i2}, \dot{x}_{i2})$, τ_{if} , and F_{ihef} , respectively. Furthermore, one has

$$\begin{cases} k\dot{x}_{i2f} = \text{sig}(x_{i2} - x_{i2f})^{\rho_1}, \\ k\dot{Y}_{if}(x_{i1}, x_{i2}, \dot{x}_{i2}) = \text{sig}(Y_i(x_{i1}, x_{i2}, \dot{x}_{i2}) - Y_{if}(x_{i1}, x_{i2}, \dot{x}_{i2}))^{\rho_1}, \\ k\dot{\tau}_{if} = \text{sig}(\tau_i - \tau_{if})^{\rho_1}, \\ k\dot{F}_{ihef} = \text{sig}(F_{ihe} - F_{ihef})^{\rho_1}, \end{cases} \quad (\text{B2})$$

where $x_{i2f}(0) = 0$, $F_{ihef}(0) = 0$, $Y_{if}(x_{i1}(0), x_{i2}(0)) = 0$, and $\tau_{if}(0) = 0$.

Then \dot{x}_{i2f} can be replaced by $\frac{\text{sig}(x_{i2} - x_{i2f})^{\rho_1}}{k}$.

To remove the previous PE condition for system signals, we introduce a matrix $H_i(t)$ and a vector $D_i(t)$. By applying the developed nonlinear filter, the tuning laws of $H_i(t)$ and $D_i(t)$ are designed as

$$\begin{cases} \dot{H}_i = -\ell H_i + Y_{if}^T(x_{i1}, x_{i2})Y_{if}(x_{i1}, x_{i2}), & H_i(0) \geq \sigma I, \\ \dot{D}_i = -\ell D_i + Y_{if}^T(x_{i1}, x_{i2})(\tau_{if} - Y_{if}(x_{i1}, x_{i2}, \dot{x}_{i2})\Theta_i + F_{ihef}), & D_i(0) \geq \sigma I, \end{cases} \quad (\text{B3})$$

where $\ell \in \mathbb{R}_+$ representing a forgetting factors for the filter matrix is chosen as a positive constant. Additionally, the dynamic behavior of the $H_i(t)$ and $D_i(t)$ can be determined by selecting different ℓ .

Considering an integral duration $T_d \in \mathbb{R}_+$, by integrating (B.2) in this period, it can be obtained that

$$\begin{cases} H_i(t) = \int_{t-T_d}^t e^{-\ell(t-v)} Y_{if}^T(v) Y_{if}(v) dv, \\ D_i(t) = \int_{t-T_d}^t e^{-\ell(t-v)} Y_{if}^T(v) [\tau_{if}(v) - Y_{if}(v)\Theta_i + F_{ihef}(v)] dv. \end{cases} \quad (\text{B4})$$

According to (A3), the IE condition for the system signal can be understood as $H_i(T_d) \geq \sigma I$, where σ is a signal exciting strength. σ can be obtained by finding the minimal singular value of $\int_{t-T_d}^t e^{-\ell(t-v)} Y_{if}^T(v) Y_{if}(v) dv$. Let T_e be the first epoch that satisfies the IE condition [20]. Then, define a current maximal exciting strength as follows:

$$\sigma_c(t) := \max_{r \in [T_d, t]} \{\sigma(r)\}. \quad (\text{B5})$$

The vector $W_i(T_e)$ applied in the new parameter adaptive law (22) can be derived with $H_i(T_e)$, $D_i(T_e)$ as

$$W_i(t) = \begin{cases} H_i(T_e)\theta_i - D_i(T_e), & t \geq T_e, \\ 0, & \text{otherwise.} \end{cases} \quad (\text{B6})$$